

**Sources of post-orogenic calcalkaline magmas: the
Arrochar and Garabal Hill-Glen Fyne complexes,
Scotland**

J. D. Clemens^{a*}, D. P. F. Darbyshire^b, J. Flinders^{c†}

*a Department of Geology, Geography & Environmental Studies, University of Stellenbosch,
Private Bag XI, 7602 Matieland, South Africa*

*b NERC Isotope Geosciences Laboratory, British Geological Survey, Keyworth, Nottingham
NG12 5GG, UK*

*c Department of Earth Sciences, University of Manchester, Oxford Road, Manchester
M13 9PL, UK*

† Deceased

* Corresponding author, *E-mail address*: jclemens@sun.ac.za

Abstract

The 425 Ma Arrochar and Garabal Hill-Glen Fyne complexes of highland Scotland are examples of post-orogenic magmatism accompanying extensional collapse of an orogen, in this case the Caledonian. The rocks are dominantly high-K series, but range from medium-K to shoshonitic. Mantle upwelling, melting and the intrusion of large volumes of mafic magma into the crust are inferred to have accompanied lithospheric thinning, and to have provided the heat source for melting of young arc crust accreted during the preceding subduction epoch. Fluids evolved from the subducting slab are inferred to have caused high degrees of enrichment in the overlying mantle wedge. Deep in the crust, the mantle-derived, K-rich mafic to intermediate magmas mixed with felsic crustal melts to form the spectrum of magmas intruded in the two complexes. Microgranular enclaves in the granitic rocks represent mafic magmas derived from the enriched mantle and hybridised by reaction, diffusion and mechanical mixing with their host felsic magmas, but they do not form part of the evolutionary series that produced the host magmas. Rather than inheriting its LILE-enriched character directly from crustal melts, or from crustal assimilation by mafic magmas, the high-K series may commonly owe at least part of its potassic character to the involvement of mantle (highly metasomatised by slab-derived fluids) as a major magma source. Enclave suites, though prominent in some granitic rocks should not be assumed to represent magmas that played a significant role in the production of the chemical variations in their host magmas.

Keywords: Medium-K; High-K; Calcalkaline; Granite; Sr-Nd isotopes; Petrogenesis; Magma mixing

1. Introduction and regional geological setting

Medium- to high-K calcalkaline and alkali-calcic igneous rocks are common in both orogenic and postorogenic settings. There has been debate about the origins of such magmas, in particular the high-K series. Proposed models involve processes such as partial melting of K-rich meta-andesites (e.g., Roberts and Clemens, 1993), reactive assimilation of metapelites by high-alumina basaltic magmas (e.g., Patiño Douce, 1995), simple mixing of felsic metasediment-derived and basaltic magmas (e.g., Davis and Hawkesworth, 1993) and melting of enriched mantle, accompanied by assimilation of crustal rocks and fractional crystallisation (e.g., Schaltegger and Corfu, 1992). Here, we present geochemical and isotope (Sr and Nd) data for a group of spatially and temporally associated mainly medium- to high-K plutonic rocks that range in composition from gabbros to granites. Our aim is to constrain the processes and materials that could have been involved in their genesis, and to present a model that may be applicable to other post-orogenic, K-enriched suites.

The Garabal Hill-Glen Fyne and Arrochar igneous complexes (ca 425 Ma) lie in the south-western Grampian Highlands of Scotland, ~ 25 km north-west of the Highland Boundary Fault (Fig. 1). They intrude Dalradian metasedimentary rocks of the Southern Highland Group. In this paper, the igneous rocks have been named according to the chemical scheme of Middlemost (1994).

The Arrochar complex (Figs 2 and 3) is crudely concentrically zoned, with a porphyritic gabbro, enclosing a small central mass of granodiorite. Minor bodies of monzodiorite occur adjacent to the granodiorite and in small isolated bodies within the main intrusion. Ultramafic rocks form linear bodies, adjacent to minor faults within the intrusion, and an igneous breccia occurs at several localities at the periphery of the main intrusion. The Ardlui gabbro is one of many, small (typically < 500 m diameter), intermediate to mafic satellitic bodies that crop out to the north-east, parallel to the long axis of the main Arrochar intrusion. The Garabal Hill body lies roughly parallel to and ~ 7 km to the north of Arrochar, adjacent to the Garabal

Fault, which produced an apparent sinistral displacement of ~ 3 km in the body (Figs 2 and 4). All the rock-types at Arrochar also occur at Garabal Hill, but there is no zoning or other discernible pattern in their distribution. The rocks crop out as irregular-shaped masses of various sizes, on both sides of the fault. Glen Fyne is dominated by a fairly homogeneous granite with large K-feldspar phenocrysts, forming the central part of the intrusion (Figs 2 and 4). The margins are more diverse in composition, with granodiorites, quartz monzonites and monzonites, in addition to the granite. Small bodies of pegmatite, leucogranite and granophyre occupy the highest topographic levels.

There have been relatively few published accounts of the petrology of the Arrochar and Garabal Hill-Glen Fyne intrusions since the work of Anderson (1935) on Arrochar and the pioneering study of Nockolds (1941), which addressed the origin of the Garabal Hill-Glen Fyne complex. Johnston and Wright (1957) described the geology of the tunnels of the Loch Sloy hydroelectric scheme. Summerhayes (1966) used the Rb-Sr method to date Garabal Hill, and Rogers and Dunning (1991) used zircon and titanite U-Pb ages to constrain the emplacement age of the Garabal Hill-Glen Fyne complex.

As is common in high-level, dominantly granitoid intrusions, the rocks contain dark-coloured, microgranular enclaves. There are, however, no large concentrations of these enclaves, which are generally found sparsely scattered throughout the host granitoids. The textural, mineralogical and chemical characteristics of these (see e.g., Vernon, 1990) indicate a magmatic origin. Flinders and Clemens (1996) examined enclave spatial distribution, textures, host-enclave interface topographies and major-, trace-element and isotope chemistries, to assess their role in the petrogenesis of the rocks. Their main conclusion was that enclave suites, with varied chemical and isotopic characteristics, within a single host felsic rock, could represent different stages in the temporal evolution of a complex magma system, driven by non-linear dynamics. Here we re-examine the enclave data, mainly in the context of the origin of the rest of the rocks in the area.

2. Previous isotope research

Stephens and Halliday (1984) subdivided the Scottish Caledonian granites into three suites: the Argyll, Cairngorm and South Grampian Suites. Relative to the others, the rocks of the South Grampian Suite, which includes the present study area, have substantially lower Ba, Sr and Na contents and more radiogenic Nd ($\epsilon_{\text{Nd}} < -6$), reflecting a difference in magma sources. From a Sr isotope study on Garabal Hill, Summerhayes (1966) concluded that there are fundamental differences in isotopic character between rocks within the complex, and ascribed these differences to local magma contamination.

The K-Ar biotite date of 412 ± 10 Ma (Harper, 1967) provides a minimum age for a coarse-grained diorite. Based on a whole-rock Rb-Sr analysis, Harmon and Halliday (1980) obtained an initial $^{87}\text{Sr}/^{86}\text{Sr}$ ratio for Garabal Hill of 0.70741 ± 7 , using an age of 406 Ma, and also measured a whole-rock $\delta^{18}\text{O}$ value of 10.4 ‰. A statistically significant positive correlation between initial $^{87}\text{Sr}/^{86}\text{Sr}$ and $\delta^{18}\text{O}$, among the late-Caledonian granites, led Harmon and Halliday to suggest that a major petrogenetic process must be involved. They ruled out differential partial melting of a single source and derivation from a single parental melt, because of the wide variations in $\delta^{18}\text{O}$ both within and between plutons. Harmon and Halliday concluded that the late Caledonian granites were derived from variable-ratio mixtures of mantle and/or mafic lower crustal source materials, with some influence of local, upper continental crust. The inference of multiple magma sources is supported by the work of Appleby et al. (2006), who concluded that more than one magma source is required to explain the zircon isotope data.

Halliday (1984) reported an ϵ_{Nd} of -3.7 for Garabal Hill. He plotted ϵ_{Nd} against $\delta^{18}\text{O}$ (from Harmon and Halliday, 1980) and showed that granites with inherited zircons and with $\epsilon_{\text{Nd}} < -6$ may not have undergone any greater degree of crustal ‘contamination’ than those with more radiogenic Nd signatures and without inherited zircons. Harmon and Halliday had

suggested that the magmas with more evolved isotope signatures may have formed either by partial melting or by assimilation of older crust. They proposed that the Garabal Hill magma might have interacted with young, continental crust, to produce its $\delta^{18}\text{O}$ signature. U-Pb analysis of inherited zircons from the Caledonian granites give upper intercept ages of ~ 1600 Ma, which suggests that primary Grenvillian-age crust (1 Ga) need not be present (Pidgeon and Aftalion, 1978). A southerly-derived component of young accreted arc, trench and oceanic fragments would explain most of the isotope data.

Rogers and Dunning (1991) obtained high-precision U-Pb isotope analyses of two titanites from a pegmatoidal quartz monzodiorite from Arrochar, yielding an age of 426 ± 3 Ma. They also dated zircon and titanite from a Garabal Hill coarse-grained diorite. Based on the near-concordance of the zircons, the uniformity of the $^{207}\text{Pb}/^{206}\text{Pb}$ ages, and the fact that the pluton cooled through the closure temperature of titanite (~ 625 °C) at 422 ± 3 Ma, Rogers and Dunning concluded that the age of this diorite is 429 ± 2 Ma. In the light of all these results we adopt an age of 425 Ma for the Arrochar and Garabal Hill-Glen Fyne intrusive complexes.

3. Potential magma sources in the crust and mantle

Steinhoefel et al. (2008) studied the Nd isotope characteristics of a number of Scottish Caledonian granitic intrusions. They concluded that, here, granitic magmas of the age of Arrochar and Garabal Hill-Glen Fyne were associated with juvenile mantle-derived additions to the crust together with recycling (melting) of young arc crust that had formed at an Andean margin, during the collision of Laurentia and Baltica. At the time of felsic magma genesis, sinistral transtension is inferred to have involved lithospheric thinning and melting of the upper mantle. The intrusion of large volumes of hot mafic magma into the deep crust would have provided a heat source to cause crustal melting. Thus, felsic magmas that formed parts of the intrusive complexes in the study area, particularly the Garabal Hill-Glen Fyne complex,

could potentially represent the products of high-degree fractionation of the mantle-derived mafic magmas (e.g. Sisson et al., 2005; Whitaker, 2008), or they could represent crustal melts, with or without mixtures of mantle components. Below, we review the evidence for the types of basement materials that might be present in the deep crust of the region.

The nature of the lower crust (potential source rocks for some felsic magmas) beneath Grampian Scotland is much debated. The lithosphere in the north and west of Scotland contains mantle seismic reflectors that result from several major deformation events during the past 1 to 3 Gyr. Northwest of the leading edge of the Moine Thrust, rocks of the Laurentian foreland crop out both on the Scottish mainland and in the Outer Hebrides. The Lewisian gneisses of this foreland have Archaean protoliths that have been affected by several, subsequent, high-grade metamorphic and deformation events (Lyon and Bowes, 1977; Kinny and Friend, 1997; Park and Tarney, 1987; Cliff and Rex, 1989; Friend and Kinny, 1995; Friend and Kinny, 2001; Kinny and Friend, 2005). The occurrence of 1.08 Ga eclogites at Glenelg implies that the Caledonian in the northwest experienced crustal thickening by imbrication (Sanders et al., 1984). Conversely, Halliday et al. (1985) and Halliday (1984) proposed that, during the final stages of the closure of the Iapetus Ocean, a basement comprised of early Palaeozoic crust was thrust to the northwest. Thus, the deep Grampian crust could contain Lewisian, Grenvillian and Caledonian rocks. There may also be a rock layer below the Lewisian, with a density consistent with granulite-facies intermediate to felsic rocks (Bamford et al., 1978). Evidently, the crust below the Grampian terrane is potentially highly complex. We shall return to this subject in the discussion section, in the context of the isotope data presented here.

The combined U-Pb geochronology, REE- and trace-element analysis, and O and Hf isotope analysis of zircons in two Caledonian granites (Appleby et al., 2006) has been interpreted as requiring multiple magma sources for both granites, including both mantle-derived and crustal components. The mantle here has also potentially been reworked

tectonically, in multiple events, and significantly enriched by fluids derived from subduction related to the closure of the Iapetus Ocean. Menzies and Halliday (1988) summarised the data from the mostly mafic, granulite-facies, meta-igneous xenoliths found in Scottish Tertiary basalts. These xenoliths have Sr and Nd isotope characteristics that suggest that the subcontinental mantle beneath this part of Scotland has characteristics similar to the enriched mantle reservoirs EM1 and EM2, as well as even more enriched rock types (Zindler and Hart, 1986; Chauvel et al., 1992).

4. New samples analysed for Rb-Sr and Sm-Nd isotopes

The Arrochar samples represent the three major rock types present – porphyritic gabbro (ARR 04.90/3), diorite (ARR 09.89/11) and granodiorite (ARR 09.89/20). A gabbro from the outlying Ardlui intrusion (ARD 09.89/2), a monzodiorite (ARR 04.90/5) and its gabbroic diorite enclave (ARR 04.90/5), and a gabbroic diorite dyke (ARR 10.90/19) from south of the main intrusion complete the set. Two samples from Garabal Hill were selected, a granodiorite (GH 04.90/20) and a diorite enclave (GH 04.90/18) from immediately to the north of the Garabal Fault. Twelve rocks were analysed from the Glen Fyne complex, covering a wide variation in major-oxide and trace-element contents and textural types (e.g., granites GF 10.90/10, and GF 12.89/2, granodiorite GF 10.90/15, quartz monzonite GF 06.91/9 and monzonite GF 10.89/6). Twelve microgranular enclaves were also selected, and range in composition from syenite (GF 10.90/5) to gabbroic diorite (GF 12.89/12B). Several enclaves were analysed together with their host rocks, for comparison purposes. Appendix B shows which enclave samples relate to which host rocks. The Dalradian here is a monotonous sequence of pelitic to semi-pelitic metasediments of regionally uniform composition. The Dalradian country-rock schist sample (GF 07.91/5) is considered representative, and was taken from just south of the Glen Fyne intrusion.

Eight samples collected by the British Geological Survey for scientific research on gold metallogenesis in the Dalradian of Scotland were also analysed, to augment the sample suite analysed by the late Dr Jim Flinders. These samples are a fine-grained ultramafic rock (DRR 132) and a monzodiorite (DRR 129.2) from Garabal Hill and five samples from satellite bodies of Arrochar at Inversnaid and Glen Gyle, ranging in composition from gabbroic diorite (DRR 103 and DRR 108), diorite (DRR 110) and monzodiorite (DRR 112) to granodiorite (DRR 115).

4.1. Petrography

The porphyritic gabbro (ARR 04.90/3) has pyroxene glomerocrysts in a groundmass of mostly fresh, flow-aligned plagioclase tablets. The glomerocrysts have cores of orthopyroxene rimmed by clinopyroxene, in turn rimmed by hornblende, with patchy replacement by biotite. Some of the plagioclase is altered to sericite. The amphibole-phyric diorite (ARR 09.89/11) contains glomerocrysts of hornblende in a medium-grained felsic matrix. Rare, earliest formed, calcic pyroxenes are partially pseudomorphed by hornblende. In the Arrochar central granodiorite (ARR 09.89/20) plagioclase tablets formed a framework within which quartz phenocrysts and fine-grained mosaic quartz crystallized. The feldspars show some alteration to muscovite, sericite and epidote, and the biotite is commonly partially altered to chlorite. The medium-grained Arrochar monzodiorite occurs as dykes within the porphyritic gabbro, close to the central granodiorite, and is rich in small, mafic enclaves (ARR 04.90/5 host and enclave). It contains altered plagioclase, interstitial quartz, a few pyroxenes rimmed by hornblende, and rare glomerocrysts of pyroxene partially replaced by hornblende. The enclaves have fine-grained matrices of altered plagioclase, hornblende and pyroxene, with rounded phenocrysts of these same minerals.

Despite their proximity, the Garabal Hill felsic rocks are unlike any from Glen Fyne. The granodiorite (GH 04.90/20) has neither the mineralogy nor the texture typical of a

granitoid. It contains fresh, flow-aligned, subhedral plagioclase tablets, scattered hornblende glomerocrysts and flow-aligned hornblende prisms and minor interstitial biotite and quartz. The dioritic enclave from this granodiorite (GH 04.90/18) contains rare K-feldspar and more common plagioclase phenocrysts in a matrix dominated by randomly orientated plagioclase tablets and interstitial quartz, with subhedral biotite and hornblende. There was some pyroxene, now pseudomorphed by hornblende.

The K-feldspar-phyric granite (GF 12.89/2) is the typical Glen Fyne felsic rock. Here, plagioclase forms glomerocrysts and individual crystals in a mosaic dominated by K-feldspar and quartz. The granite (a microgranite in hand specimen, GF 10.90/10) has scarce plagioclase and more abundant orthoclase and quartz phenocrysts in a groundmass of equigranular K-feldspar, plagioclase, mafic minerals and quartz. The quartz monzonite (GF 06.91/9) has a distinctive texture, and a modal mineralogy dominated by plagioclase, hornblende and biotite. Hornblende and biotite occur both as numerous glomerocrysts and separate euhedra. K-feldspar occurs only as scarce megacrysts. Hornblende, biotite and titanite form small euhedra, with rare interstitial quartz.

Glen Fyne enclaves are fine-grained and equigranular, containing K-feldspar, plagioclase and quartz xenocrysts, commonly with reaction rims of mafic minerals. Engulfed lobes, veins and stringers of granite also occur inside the enclaves, and some contain coarse-grained euhedral biotite with the same chemistry as that in the host granites. These enclaves also commonly contain pseudomorphs after pyroxene and rarely after olivine. The pseudomorphs, and the high Mg numbers [$100\text{Mg}/(\text{Mg}+\text{Fe})$] of the rocks, typically ~ 75 in the most mafic enclaves, show that the initial enclave magmas were mafic.

5. Whole-rock geochemistry

Table 1 shows the major- and trace-element whole-rock analyses of the new samples from the various intrusions described above. A much larger number of rocks were analysed

for major and trace elements than for the radiogenic isotopes. The whole-rock geochemistry provides some preliminary constraints on possible models for petrogenesis of the magmas. These models are then tested and refined using the isotope data. Appendix C contains details of the whole-rock analytical methods.

5.1. Variation diagrams

The suite is generally metaluminous, with the great majority of the analysed rocks having ASI (Alumina Saturation Index = mol. $\text{Al}_2\text{O}_3/[\text{CaO}+\text{Na}_2\text{O}+\text{K}_2\text{O}] < 1.1$, and would be classified as I-type, in the scheme of Chappell and White (1974, 2001). On the K_2O - SiO_2 diagram of Le Maitre et al. (1989), a large proportion of the analysed rocks plot as high-K series. As an example, Figure 5 shows this plot for the Glen Fyne pluton, omitting the three ultramafic rocks (GF 04.90/3A, GF 04.90/3A(alt) and GF 04.90/4, Table 1). Here, the largest group of analyses plot as high-K series but a significant number plot in both the medium-K and shoshonitic fields, and two plot as low-K rocks. The enclaves from the Glen Fyne complex are also variable, again mostly high-K but with a similar proportion of data points in the medium-K and shoshonitic fields, forming a broad subvertical array, along with the low- SiO_2 group of host rocks (Fig. 5a). The Arrochar rocks are mostly medium-K, with a significant number also plotting as high-K. Using the classification of Frost et al. (2001) the rocks all belong to the magnesian series. On the modified alkali-lime index (MALI = $\text{Na}_2\text{O}+\text{K}_2\text{O}-\text{CaO}$ by wt) plot (Fig. 5b) the Glen Fyne rocks plot span the calcic to alkalic fields, with the majority being alkali-calcic. The Glen Fyne enclaves plot approximately equal numbers in the alkalic and alkali-calcic fields. Arrochar rocks, like those from Glen Fyne, span the entire spectrum, from calcic to alkalic, but with the majority plotting in the calcic to calc-alkalic fields. Garabal Hill rocks are alkali-calcic to calc-alkalic.

According to Frost et al. (2001) rocks from a pluton, or genetically related plutons, normally plot within a narrow band on the SiO_2 vs MALI diagram, essentially within the band

for a given series. Clearly the rocks of this area do not obey this rule. Furthermore, the different series identified by Frost et al. are commonly given tectonic significance. For the magnesian series, calcic rocks are said to typify island arcs and plutons emplaced in the outboard parts of cordilleran arcs. The calc-alkalic series are identified with the main cores of cordilleran arcs. The alkali-calcic series are said to occur in the inboard sections of cordilleran arcs and in plutons associated with delamination of overthickened crust. Finally, the alkalic series is supposed to occur in the inboard sections of arcs. Clearly, the magmas of area under discussion cannot have been produced in all these settings simultaneously, so it seems questionable to attribute tectonic significance to these different types of magma chemistry.

As pointed out by Roberts and Clemens (1993) magmas differentiating by crystal fractionation tend to produce rock series that plot on the $\text{SiO}_2\text{-K}_2\text{O}$ diagram without crossing the boundaries between the different series, except where the magmas are initially transitional in chemistry. This is similar to the normal behaviour in the $\text{SiO}_2\text{-MALI}$ plot. The fact that the Glen Fyne rocks, for example, plot across several of these fields, in arrays with steep slopes rather than subparallel to the series boundaries, strongly implies that either magma mixing processes were involved, or that there were multiple magma sources and the trends do not reflect a differentiation process. This is not to imply that differentiation did not occur, but that the main geochemical trends appear to have another origin (see also Clemens et al., 2009).

Figure 6 shows multi-element diagrams normalised to primitive mantle concentrations. These plots show the variation for all rocks for which there is a complete set of analyses. The main magmas in the suite have negative Nb anomalies indicating the involvement of crustal materials in their formation. The patterns for the rocks of Glen Fyne (Fig. 6a), Garabal Hill (Fig. 6b) and Arrochar (Fig. 6c) are all very similar. The only rock that shows a markedly different pattern is Glen Fyne granite sample GF 02.92/24, which has a steeper profile with progressive depletion in the more compatible elements and particular negative anomalies in Ce, P and Ti. This is the most felsic rock plotted (76.86 wt% SiO_2 , Table 1) and suggests that

it could represent a highly differentiated magma. However, as will be seen later, this rock has Sr and Nd isotope characteristics that rule out an origin by crystal fractionation. These diagrams also show that even the mafic rocks commonly have high LIL element (Rb, Ba and K) contents (mostly 100 to 300 times primitive mantle), similar to the upper continental crust. This suggests that the presumed mantle sources for the more mafic magmas in the suite must have been highly enriched, either as a primary characteristic or through crustal assimilation. Enclave magmas (Fig. 6d) are rather similar but many have very small negative Nb anomalies, implying less crustal involvement in their genesis. These features imply that the mafic end-members of the enclave suite were produced by partial melting of mantle rocks in a setting other than subduction, consistent with the post-orogenic timing of the magmatism. Overall, the suite has geochemical features indicating magma sources in the highly enriched continental mantle and in the crust.

Figure 7 shows Harker plots for Al_2O_3 , CaO, MgO and Sr. These oxides and elements exemplify the types of trends shown by all the others in the dataset. At the outset it should be noted that the rocks of the Glen Fyne complex plot in two distinct areas on these diagrams. There are high- SiO_2 and low- SiO_2 groups, with a discontinuity (SiO_2 gap) between them. Due to the large number of rocks plotted from Arrochar and Garabal Hill, and the necessarily compressed SiO_2 axes, this feature of the Glen Fyne data is not obvious in most of the plots. However, in Fig. 7c, for Sr, the gap is more apparent because of the switch from crudely positive correlation of Sr with SiO_2 in the low- SiO_2 group to a subvertical array in the high- SiO_2 group.

The Al_2O_3 trend (Fig. 7a) is similar to that for P_2O_5 , V, Zr, Nb, Ce and Nd. It is essentially a relatively tight, hump-shaped trend that resembles the sort of variation produced by fractionation of a mafic magma. However, for Al_2O_3 , there is a marked discontinuity between this trend and a group of mafic to ultramafic rocks with very low Al_2O_3 contents. This discontinuity is far less prominent for most of the other elements in this grouping. Figure

7b shows the variation for CaO, which is very similar to those for FeO* (total Fe as FeO) and TiO₂. These oxides form relatively tight negative arrays, but CaO and TiO₂ both show a few anomalously low concentrations, particularly in some of the very mafic rocks. Figure 7c shows the variation in MgO. The negative curvilinear shape suggests fractionation from a mafic parent for much of the series. However, there is a group of low-SiO₂ rocks with markedly higher MgO contents, creating a discontinuity and suggesting the presence of more than one parent magma. The variation shown by Sr, in Figure 7d exemplifies the type of variation also shown by Na₂O, Rb, Y, Ba and La. These elements form two distinct clusters within each of which there is a large degree of scatter. As noted above, the cluster with SiO₂ < 63 wt% shows a crude positive correlation with SiO₂, while that with SiO₂ > 63 wt% shows an equally crude roughly vertical scatter.

There are several things to note here. The first is that, in felsic rock series produced by fractionation involving plagioclase, Sr generally mirrors the behaviour of CaO, since a large proportion of the Sr in the rock resides in the plagioclase. However, comparison between Figures 7b and d shows that there is very little similarity in the behaviour of these two elements for this group of rocks. The second observation is the great degree of scatter in the variations for elements like Sr. For example, at about 68 wt% SiO₂, Sr varies over a factor of 500%, from ~ 270 to ~ 1400 ppm. This would be very difficult to explain in any model of differentiation from a single parent magma. Along with the grouping of the analyses into at least two clusters with differing trends, this implies that contrasting magma batches were involved in the formation of these complexes. The scatter within each grouping further suggests that the different magma batches may have inherited considerable internal heterogeneity from their protoliths. Elements such as Ca behave in the expected manner because common minerals (e.g., Pl) in the partially melted source rocks control the concentrations of such elements in the melts through element partitioning relationships. Certain trace elements, such as the alkaline earths, appear to be decoupled from the related

major elements because their concentrations in the melts are controlled by local variations in the trace-element contents of the source rocks, rather than by the minerals participating in the melting reactions. For instance, parts of a meta-andesitic source could have higher Sr contents than other parts. Melting of this package of rocks would produce magmas with similar CaO contents (controlled by equilibrium with Pl, Hbl and Cpx). However, different melt batches, from different parts of the source, could have very different Sr contents (controlled only by Sr solubility in the melts). In addition, there is a growing body of evidence that disequilibrium processes control the contents of many trace-elements and isotopes in melts, especially during partial melting of crustal rocks (e.g., Sawyer, 1991; Watt and Harley, 1993; Barbero et al., 1995; Bea, 1996; Davies and Tommasini, 2000; Janák et al., 2001). Melt batches withdrawn from a source more rapidly could inherit much lower trace-element concentrations than batches that remained longer in the source, in contact and progressively equilibrating with the minerals that host these elements.

6. Rb-Sr and Sm-Nd isotope geochemistry

Rb-Sr and Sm-Nd analytical data, with calculated initial ratios and T_{DM} model ages, are presented in Table 2, and the analytical methods described in Appendix C. Note that the concentrations of Rb, Sr and Nd given in Table 1 were obtained using the XRF at Manchester. For internal consistency, these values have been used in all the plots involving these elements, as discussed above in the section on whole-rock chemistry. Table 2 contains analyses of these elements for the samples used for isotope geochemistry. These were obtained, at NIGL, by XRF (Rb and Sr) and isotope dilution (Sm and Nd) and are of superior quality. Again, for internal consistency, the NIGL values have been used in any graphs involving these elements together with their isotopes.

6.1. Results

Most of the more felsic Glen Fyne rocks (granites and quartz monzonites) have initial Sr isotope ratios at 425 Ma ($^{87}\text{Sr}/^{86}\text{Sr}_{425}$), ranging from 0.70411 to 0.70444. However granites from the eastern part of the intrusion, GF02.92/24 and GF10.90/10, have values of 0.70507 and 0.70598 respectively, indicating a more evolved magma component. The intermediate to mafic rocks (monzonites, monzodiorites and gabbroic diorites) have more radiogenic signatures (0.70568 to 0.70672) than the felsic rocks. The intrusion is not isotopically zoned, except that the margins are more isotopically diverse than the core of the intrusion, reflecting the previously noted diversity in rock type at the margins. The Glen Fyne enclaves (with ~ 52 to 62% SiO_2) have initial $^{87}\text{Sr}/^{86}\text{Sr}$ values (0.70418 to 0.70598), comparable to those of their felsic hosts. The Garabal Hill intermediate to mafic rocks have initial $^{87}\text{Sr}/^{86}\text{Sr}$ ranging from 0.70752 to 0.70765. The ultramafic rock (DRR 132, with 0.71017) has a very low concentration of Rb and its initial ratio is suspect. The Garabal Hill enclave (GH04.90/18) has a value of 0.71024. The range of initial $^{87}\text{Sr}/^{86}\text{Sr}$ values for the Arrochar rocks is 0.70732 to 0.71145, with the highest values in the rocks with about 55% SiO_2 , while both more mafic and more felsic rocks have lower initial ratios. The Ardlui gabbro (ARD09.89/2) has an initial $^{87}\text{Sr}/^{86}\text{Sr}$ (0.70755) similar to the mafic rocks of Arrochar and Garabal Hill.

When the initial ratios are plotted against SiO_2 concentration (Fig. 8) a rather surprising trend emerges in each group. Between 55 and 70% SiO_2 the initial $^{87}\text{Sr}/^{86}\text{Sr}$ ratio decreases with increasing silica content, whereas above and below these SiO_2 concentrations the isotope ratios correlate positively with SiO_2 . The second surprising feature of these data is that some of the more mafic rocks, with $\text{SiO}_2 \sim 55$ wt%, are the most isotopically evolved rocks analysed. In contrast to what should occur in a series of rocks produced by differentiation from a single parent magma, the points for the main rock series do not define horizontal arrays. The exception is the suite of enclaves from the Glen Fyne granite, though other geochemical features rule out such an origin for these too.

Figure 9a shows an isotope correlation diagram (ϵ_{Nd} vs initial $^{87}\text{Sr}/^{86}\text{Sr}$) for the studied rocks. There is a larger variation in ϵ_{Nd} within the Arrochar suite (-5.5 to -0.4) than in the Glen Fyne host rocks (-3.2 to -1.1), suggesting greater heterogeneity in the magma sources. The Glen Fyne enclaves are generally more primitive (-1.7 to +0.5) than their hosts. Granodiorite GH04.90/20, with $\epsilon_{\text{Nd}_{425}}$ of -3.1, is the most evolved Garabal Hill rock; the other rocks plot closer to the $\epsilon_{\text{Nd}} = 0$ line. One Arrochar rock plots just below, the $\epsilon_{\text{Nd}_{425}} = 0$ line, at -0.4) while the rest have rather more negative values (-5.5 to -1.9). The points for enriched mantle melts (EM1 and EM2) are also shown on this figure, along with a point (AB) representing an average continental alkali basalt (derived using the EarthChem database; www.earthchem.org). The great majority of points for the rocks of the study area define a broad trend extending from enriched mantle toward more crustal materials, such as GLOSS (GLObal Subducting Sediment) and the schist sample that represents the country rock into which the Glen Fyne granites were intruded. The Nd isotope data for the schist sample GF07.91/5 ($\epsilon_{\text{Nd}_{425}} = -12.0$, Table 2) is within the range of values obtained for the Southern Highland Group of the Dalradian (-10.4 ± 3.3 , Evans, 1999). Figure 9b shows the data for the rocks of the study area as well as fields that closely approximate the areas in which a variety of potential basement rocks plot. These are discussed later, in connexion with the origins of the crustal components in the magmas and assimilation models.

The Arrochar and Garabal Hill enclaves have more radiogenic initial Nd isotope signatures ($\epsilon_{\text{Nd}_{425}} = -3.1$ and -1.9 respectively) than their host rocks (-4.3 and -3.1). The initial $^{87}\text{Sr}/^{86}\text{Sr}$ ratio for the Arrochar enclave is also more radiogenic, whereas the Garabal Hill enclave appears to be less evolved than its host. Many of the Glen Fyne enclaves have $\epsilon_{\text{Nd}_{425}}$ values that are within error of the values for their host rocks, although GF04.90/16B and C, GF10.90/5 and GF06.91/7F display a systematic difference of about +1 epsilon unit. Of the four enclaves GF 06.91/B, D, E and F, the largest difference in initial $^{87}\text{Sr}/^{86}\text{Sr}$ ratio is shown by GF 06.91/D, which has $\epsilon_{\text{Nd}_{425}}$ indistinguishable from that of the host rock (GF

06.91/7F). This is surprising, as the Sr isotope system will re-equilibrate more readily than that of Nd. The best interpretation of this is that the ϵ_{Nd} values of the two magmas were always similar and that this enclave cannot have resided in the host magma long enough for Sr isotope re-equilibration.

7. Discussion

7.1. Mantle and crustal components and their origins

The isotope correlation diagrams of Figure 9 show the Arrochar and Glen Fyne data, together with points for depleted mantle DM (Rehkamper and Hofmann, 1997), enriched mantle EM1 and EM2, average continental alkali basalt, Dalradian Schist (from the present study) and areas for various candidate basement rock series – Dalradian, Rhinnian, and Lewisian rocks; from Evans 1999, Morton and Taylor (1991), Marcantonio et al. (1988), Dickin and Bowes (1991) and Chambers et al. 2005. The bulk-Earth value is for CHUR at 425 Ma, and initial $^{87}\text{Sr}/^{86}\text{Sr}$ is 0.704 at 425 Ma. The data distribution in Figure 9 makes it improbable that two-component mixing of depleted mantle and either Lewisian or Dalradian crust could have produced the rocks of the Arrochar and Garabal Hill-Glen Fyne complexes. A plot of initial Sr and Pb isotope ratios, at *ca* 420 Ma, for other Caledonian granites (Dickin and Bowes, 1991) shows distributions of points very different to those for the Lewisian complex or the Grampian Dalradian. The Dickin and Bowes plot also shows near coincidence of data from several Caledonian granites and the west Islay-Colonsay (Rhinnian) basement. Data from Caledonian granites on ϵ_{Nd} vs initial $^{87}\text{Sr}/^{86}\text{Sr}$ plots (Frost and O’Nions, 1985; Dickin and Bowes, 1991, and this work) fall between the depleted mantle end-member and average Rhinnian basement values. All this suggests the possibility of involvement of Rhinnian-type crust in the genesis of the magmas. However, it rules out generation of the magmas by simple partial melting of any of the basement materials that could be present in

the region. None of the Glen-Fyne and Arrochar magmas were produced as melts of basement crust.

From the major- and trace-element compositions of the rocks, and the various isotope diagrams presented above, it is clear that there is a strong mantle component to the rocks of the study area. Enriched mantle EM1 has a very similar ϵNd_{425} and T_{DM} model age (-2.0 and 1.32 Ga) to the main series of felsic Glen Fyne rocks. Thus it may well be that these magmas were produced by partial melting of K-rich mafic rocks that crystallized from magmas not long before 425 Ma. It also seems most likely that production of the rock series has involved mixing between mantle and crustal magma components. This is most obvious in plots such as Figures 8 and 10. An important issue is the nature of the crustal component in these magmas and the mechanism of its introduction. Possibilities include assimilation of crustal rocks by mantle-derived mafic magmas, mixing between crustal melts and mantle magmas, and melting of variably enriched mantle. Another major issue is whether the more felsic magmas were produced by fractionation of the mafic magmas or produced independently, and related to each other and the mafic magmas only by (inefficient) mixing processes.

7.2. Assimilation models

Various types of assimilation models are commonly used to explain geochemical variations in igneous rock suites. Recent variants include the energy-constrained assimilation and fractional crystallisation model of Spera and Bohrson (2001) and the reactive bulk assimilation mechanism proposed by Beard et al. (2005). For the present rock suites, Figure 9 suggests a model in which a mantle-derived mafic magma (perhaps similar to the average alkali basalt plotted in Figure 9a) assimilated Dalradian country rocks, to produce part of the observed variation. Involvement of Lewisian tonalite-trondhjemite-granodiorite series (TTG) rocks and Rhinnian basement seems unlikely. However, the analysed country-rock Dalradian schist plots in an appropriate area of the diagram. Even though, at emplacement level,

assimilation has not occurred, this process could conceivably have occurred at depth. The position of GLOSS also suggests that material such as this could be involved as an assimilant. The positions of points in Figure 8 are also compatible with assimilation of GLOSS-like material or Dalradian schists by a mafic magma derived from the enriched mantle.

Bulk assimilation models can be tested using the isotope constraints. We carried out Sr isotope mixing calculations using EM2 melt ($\text{SiO}_2 = 46.82$ wt%, Sr = 333 ppm, initial $^{87}\text{Sr}/^{86}\text{Sr} = 0.7067$) as the assimilating magma and a variety of possible bulk assimilants. From Figures 8 and 9a it is clear that we need to explain the trend from the compositions of enriched mantle melts, such as EM1, EM2 or AB / GAB, to the strongly evolved crustal signature of mafic rocks like DRR103 (Tables 1 and 2). The target composition is calculated as the average of three Arrochar dioritic rocks with the highest $^{87}\text{Sr}/^{86}\text{Sr}_{425}$ ($\text{SiO}_2 = 56.22$ wt%, Sr = 447 ppm and $^{87}\text{Sr}/^{86}\text{Sr}_{425} = 0.7111$). Assimilation of 51% of the analysed Dalradian schist would shift the initial $^{87}\text{Sr}/^{86}\text{Sr}$ of the magma to the target value, and the SiO_2 content would be just over 55.87 wt%, close to the target value of 56 wt%. However, this process would produce a magma with only 248 ppm Sr (just over half the target value), considerably deficient in Al_2O_3 , CaO, P_2O_5 , and far too rich in K_2O , MgO and Rb. Data for Dalradian metasediments (Evans 1999 and BGS[©]NERC unpublished data) show that these rocks all have Sr contents that are too low or $^{87}\text{Sr}/^{86}\text{Sr}_{425}$ too low (or both), requiring $\gg 50\%$ assimilation to match $^{87}\text{Sr}/^{86}\text{Sr}_{425}$, and, even then, yield products with Sr contents much lower than the target values. Similar problems rule out bulk assimilation of the 2.8 Ga TTG-series Lewisian rocks of the NW UK continental margin, the 1.75 Ga rocks of Rockall Bank and the 1.78 Ga Islay (Rhinnian) gneisses (Chambers et al 2005; Morton and Taylor, 1991; Marcantonio et al., 1988). None of the candidate basement assimilants in the region could produce a hybrid magma with the correct major-element concentrations and simultaneously satisfy the isotope and the trace-element constraints. Likewise, setting the assimilant as GLOSS would require nearly 60 wt% assimilation to realise the target $^{87}\text{Sr}/^{86}\text{Sr}_{425}$ value. Here

the SiO₂ content of the product magma would be somewhat high (nearly 58 wt%) and the Sr content would be 329 ppm, still considerably lower than the target value. The amounts of assimilation required in these models are very high. Together with the various elemental mismatches that result, this suggests that bulk assimilation models are inadequate to explain the compositions of the highly enriched mafic magmas from Arrochar. We therefore conclude that bulk assimilation of any of the present wall-rock or possible basement materials is unlikely to have exerted a major influence on the chemical and isotopic evolution of the magmas.

Assimilation involving the mixing of a mafic magma and the partial melt derived from a potential assimilant is another, perhaps more realistic, scenario. Figure 8 shows that mixing with such metasediment-derived melts could potentially explain the slope of the trend from enriched mantle melts, through the gabbros to the gabbroic diorites with elevated initial ⁸⁷Sr/⁸⁶Sr, although it can have nothing to do with any trends toward the more granitoid rocks in the suite. Plots of initial Sr isotope ratio against some major oxides (e.g. FeO*+MgO and CaO; Fig. 10) are also broadly compatible with a scheme involving assimilation of a felsic melt derived from the Dalradian schist by an alkali basaltic magma. Experiments have shown that partial melting of a wide range of crustal rock types, and particularly metasediments, produces melts with SiO₂ contents of 72 to 76 wt%, depending on melting conditions; see Moyen and Stevens (2005) for a summary. The average is 74 wt% SiO₂, so this is the assumed value for a melt derived from the analysed Dalradian schist, for example. A compilation of compositional data for 235 post-Archaean S-type granitic rocks with SiO₂ between 72 and 76 wt% (Villarsos, 2009; Villarsos et al., 2009) shows that the Sr contents of melts formed from metasediments are quite variable, ranging from 2 to 494 ppm. However, rocks with > 250 ppm Sr are exceptional, and the mode is 144 ppm – far lower than would be required (~ 500 ppm) for construction of a successful assimilation model. Production of the intermediate Arrochar magmas, with highly elevated initial Sr isotope ratios and high Sr

contents would require an unusually Sr-rich component as one end-member in whatever process brought about the variations.

Apart from the abovementioned difficulties in fitting the geochemical data to an assimilation model, recent work by Glazner (2007) has shown that bulk assimilation processes (both reactive and mechanical) are severely limited by the energy required to accomplish the hybridisation. Glazner demonstrated that hybrids could be produced with appropriate geochemical and isotopic characteristics. However, he pointed out that the hybrid magmas would be highly crystalline (50 to 70 vol.% crystals). In the present context, such a high magma crystallinity is incompatible with the textural and geological evidence for the melt-like and mobile character of the intermediate magmas from this study area, some of which occur as fine-grained dyke rocks. As shown above, any assimilation scheme applied to the present rocks would also require large amounts of assimilation (> 50 %), producing high degrees of crystallinity in the products and rendering them effectively immobile. Thus, assimilation of wall or basement rocks is unlikely to be the source of the strong enrichments observed in the more mafic Arrochar and Glen Fyne magmatic rocks. Since the more felsic magmas of these complexes have relatively primitive Sr isotope ratios – more primitive than the enriched mantle (see e.g. the plots in Figs 8 and 10), this would rule out all potential assimilants apart from the most primitive and mafic rocks of the Rhinnian basement crust (see Fig. 9b). Thus, basement rock assimilation is also unlikely to have played a role in producing the more felsic rocks of the Garabal Hill-Glen Fyne complex.

7.3. Inferences from the enclave magmas

The Glen Fyne enclave magmas cannot be the equivalents of the more mafic magmas in the complexes under consideration because many of the enclaves have significantly higher ϵNd_{425} , and all have lower $^{87}\text{Sr}/^{86}\text{Sr}_{425}$ (Figs 8 and 11). Along with much other evidence presented here, Figures 8 and 10 demonstrate that the enclaves do not form

part of the magmatic lineage responsible for the production of the main Glen Fyne plutonic magmas. From petrographic features, and Figures 8 and 11, it is clear that the enclave magmas have been hybridised by extensive diffusive exchange and subordinate mechanical mixing with their host granitoid magmas. The relatively weak negative Nb anomalies shown by the enclaves (Fig. 6d) suggest less crustal influence. Thus it seems likely that these enclaves represent small amounts of several different mafic magmas, formed by melting of the enriched mantle at 425 Ma, and either injected into, or engulfed by, the Glen Fyne felsic magmas.

The Glen Fyne isotope data also reveal statistically significant contrasts in ϵNd between host rocks and their enclaves, but there is little contrast in initial Sr isotope ratio. From the foregoing, it is clear that the present compositions of the enclaves result from mingling and mixing with their host granitic magmas. As pointed out by Beard (2008), with the evidence for the persistence of crystals from the granitic magma suspended in the enclaves, some isotopic contrasts should exist within the enclave series and between the enclaves and their host rocks. Given the petrographic evidence for chemical disequilibrium between host-derived xenocrysts and the enclave magmas, the fact that there is no significant variation in $^{87}\text{Sr}/^{86}\text{Sr}_{425}$ (see e.g. Fig. 8) has two important meanings. Firstly, the lack of contrast in $^{87}\text{Sr}/^{86}\text{Sr}_{425}$ must be a primary feature; the parent enclave magma and the host granitic magma must have had very similar $^{87}\text{Sr}/^{86}\text{Sr}_{425}$ from the outset. Secondly, the contrasts in ϵNd_{425} and the chemical disequilibrium between the enclave magmas and host minerals demonstrate that the voluminous, granitic, host magmas of Glen Fyne cannot be the residual liquids produced by fractionation of a mafic magma similar to the parent enclave liquid. This suggests an enriched mantle source for the enclave magmas and either a separate enriched mantle source or a young crustal source for the host felsic magmas.

7.4. Fractionation models

As shown above, assimilation models are inadequate to explain either the geochemical data or the textural evidence in the rocks. However, it is conceivable that the more felsic magmas could be differentiates of large volumes of mafic magmas, even though such volumes of mafic rock are not presently exposed. Sisson et al. (2005) showed that hydrous, medium- to high-K mafic magmas may differentiate to produce significant volumes (12 to 25% of the original magma volume) of granitic (s.l.) liquid. Whitaker et al. (2008) experimentally explored a similar proposition (crystallisation of hydrous olivine tholeiite) but found that extreme fractionation would be required (96 to 97 vol.%) to produce residual liquids of potassic, low-silica rhyolitic composition (≤ 68 wt % SiO_2), with the most voluminous products being intermediate in composition. The intermediate rocks of the present study area have far more evolved $^{87}\text{Sr}/^{86}\text{Sr}_{425}$ than the most felsic rocks, and so are not candidate parents. Whitaker et al. (2008) also noted the relative scarcity of intermediate progenitors to the rhyolitic and granitic rocks that they were considering, and appealed to elevated viscosity in intermediate magmas as a factor preventing their ascent. This seems unlikely, since intermediate liquids would, if anything, have lower viscosities than the rhyolitic liquids that did reach the surface and erupt. The miniscule volumes of potassic rhyolite that would be produced in the Whitaker et al. scheme suggest that the most felsic rocks of Glen Fyne are unlikely to have been formed by fractionation of a tholeiitic parent. Nevertheless, a more alkaline mafic parent magma, similar to the compositions studied by Sisson et al. (2005) remains a possibility, at least on the grounds of the relative volume of potassic rhyolite that might be produced.

The granites of the Glen Fyne complex have initial $^{87}\text{Sr}/^{86}\text{Sr}$ lower than any of the candidate mafic parent magmas in the suite (Figs 8 and 10), but similar to many of the intermediate rocks. Thus we could contemplate an origin by differentiation from intermediate parent magmas. However, there is no compositional continuum between such possible parent

rocks and these most felsic rocks. This makes such an origin less likely. Furthermore, the most felsic Glen Fyne rocks (with > 75 wt% SiO₂) also have ϵNd_{425} lower than any of the other Glen Fyne rocks (Fig. 11). Thus, it seems most likely that these felsic magmas were formed directly by partial melting of crustal source rocks, rather than by differentiation from any of the more mafic magmas. The small volume of mafic relative to felsic rocks in the area provides further supporting evidence of this.

7.5. Crustal melting and the origin of the felsic magmas

Sisson et al. (2005) suggest that partial melting of underplated arc basaltic rocks could form substantial quantities of medium- to high-K felsic magmas. The melting reactions would involve the fluid-absent breakdown of biotite and hornblende, leaving a plagioclase-enriched residue (see Clemens and Watkins, 2001). Since the setting of the Arrochar and Garabal Hill-Glen Fyne magmatism was post-subduction, we consider that the most likely origin for the felsic magmas was partial melting of relatively young arc crust of this type. This would explain why we do not see any large volumes of mafic intrusive rock emplaced in the upper crust at around 425 Ma. The small but significant degree of isotope heterogeneity among the Glen Fyne felsic rocks (e.g. Figs 8 and 10) suggests that the dominantly meta-igneous source had a variable admixture of immature sedimentary materials, possibly derived through subaerial weathering of the rocks of the precursor volcanic arc.

The felsic Glen Fyne rocks have an average $^{87}\text{Sr}/^{86}\text{Sr}_{425}$ around 0.705. If the protolith for these magmas had $^{87}\text{Sr}/^{86}\text{Sr}_{425}$ and $^{87}\text{Rb}/^{86}\text{Sr}$ similar to EM1 (~ 0.704 and 0.14), it would have to have aged approximately 70 Myr to arrive at an $^{87}\text{Sr}/^{86}\text{Sr}$ ratio of ~ 0.705. This would mean that the protolith would have to have been emplaced at about 495 Ma. The subduction that heralded the closure of the Iapetus Ocean began at about this time (Armstrong and Owen, 2001).

7.5. Origin of the crustal component in the mafic to intermediate magmas

The difficulties in explaining the geochemical and isotope data by any sort of assimilation process have been discussed above. Thus, it seems reasonable to hypothesise that the more mafic magmas of the complexes were produced by direct partial melting of very highly enriched mantle. In detail, our data suggest that the mantle sources for the more mafic rocks in the suite vary in their degree of enrichment, from ordinary enriched mantle, similar to EM1 and EM2 (Zindler and Hart, 1986; Chauvel et al., 1992), to more heavily metasomatised mantle with evolved crust-like Sr isotope signatures. We suggest that this enrichment and metasomatism is most likely to have been brought about through reactions between the mantle wedge and fluids emanating from an oceanic slab during the subduction associated with the closure of the Iapetus (which began in the Ordovician). Similar mantle wedge enrichment by slab-derived radiogenic Sr has been hypothesised for the Cascades lavas in the northwestern USA (Borg et al., 1997). Recent lithium isotope work by Elliott et al. (2006) suggests that, globally, the mantle is enriched directly by slab-derived fluids rather than by mechanical mixing with subducted crust in subduction erosion.

An important question concerns the compositions of the fluids that might be released from a descending and dehydrating slab during subduction. A related question concerns the nature of the products of reactions between such fluids and the rocks of the mantle wedge. The prevailing model is that slab-derived fluids carry significant amounts of Si, LILE, etc. to the mantle wedge at the shallower depths (e.g., Gill, 1981; Kushiro, 1990; Plank and Langmuir, 1993; Elliott et al., 1997; Tatsumi and Kogiso, 1997) and that slab melts (if they occur) may be the metasomatic agents at greater depths (e.g., Beard et al., 1993; Rapp et al., 1999; Killian and Stern, 2002; Kelemen et al., 2004), perhaps producing more sodic metasomatic products. Portnyagin et al. (2007) studied the compositions of melt inclusions in olivine crystals from volcanoes of the Kamchatka and northern Kurile Arc. They found that a solute-rich slab component dominates the budget of LILE, LREE, Th and U in the magmas.

This solute-rich component is inferred to be derived from melts or supercritical fluids derived from subducted sediments. Their calculations show that this component carried around 20 wt% K₂O and thousands of ppm of both Ba and Sr.

The experiments of Rapp et al. (1999) and the geochemical and theoretical studies of Xiong et al. (2006) suggest that fertile mantle, metasomatised by high-*T* melts, would consist of sodic amphibole pyroxenite, with phlogopite pyroxenite formed by interaction with lower-*T* melts. Kessel et al. (2005) measured the compositions of fluids and melts that had been experimentally equilibrated with a basaltic eclogite at *P-T* conditions relevant to subduction zones. At depths up to 120 km they showed that either dehydration or partial melting could occur, depending on *T*, with melts and fluids showing contrasting behaviour of U, Th, Sr, Ba, Be and LREE. However, at pressures equivalent to 180 km, even at low *T*, eclogite will coexist with a high-density, solute-rich supercritical fluid that has melt-like solubilities for these trace elements and also some major elements (e.g., Ferrando et al., 2005). At these great depths the fugitive phase, whether low-density fluid, melt or high-density fluid, would always be highly enriched in Rb and Ba. Fluid/melt-mineral partition coefficients (Kessel et al., 2005) are of the order of 100 and 40 respectively, implying efficient scavenging of these elements from the slab into the mantle. Sr is not carried into the mantle by low-density fluids at *T* < 900 °C, but is efficiently transported in the higher-*T*, low-density fluids, melts and high-density fluids, with a partition coefficient of about 20. Schmidt et al. (2004) demonstrated that subducted MORB basalts, pelites and greywackes will all develop similar eclogitic mineral assemblages and that the coexisting fluids will be rich in Si and K. Schmidt et al. (2004) and Ishikawa et al. (2005) both determined that supercritical, solute-rich fluids/melts evolved from the slab would be aqueous and strikingly enriched in B, Ba, Rb and K. It therefore seems likely that the Kessel et al. (2005) partitioning relationships will be valid for a wide range of subducted rocks.

There is evidently considerable potential for the mantle wedge to become highly enriched in K, Rb and radiogenic Sr derived from both the altered igneous and sedimentary components of a subducting slab. However, it is not possible to produce well constrained models for the resulting mantle isotope ratios (e.g., $^{87}\text{Sr}/^{86}\text{Sr}$) because the quantity of slab-derived metasomatic fluid/melt involved, and the degree of interaction with the mantle rocks, will be spatially highly variable. Nevertheless, the low Rb and Sr contents of unaltered mantle rocks mean that reaction with even small amounts of such metasomatic agents could produce crust-like isotope signatures, especially if the fluids/melts were derived from subducted sediment. Radiogenic ingrowth (ageing) would intensify this effect. Various studies (cited above) show that, unlike Rb and Sr, Nd is not efficiently carried into the mantle wedge by such fluids. Conceição et al. (2005) showed that a number of processes in subduction-zone settings are responsible for the effective decoupling of the Sr and Nd isotope systems. This contrasting behaviour of Sr and Nd is the likely explanation for the presence of some Garabal Hill and Arrochar rocks that plot just below the $\epsilon\text{Nd}_{425} = 0$ line in Figure 9a, rather than forming part of the array that extends to more crustally evolved ϵNd values, despite their elevated $^{87}\text{Sr}/^{86}\text{Sr}_{425}$. This same feature (ϵNd_{425} hovering just below 0) represents a powerful argument against bulk assimilation, as this process cannot explain the observed decoupling between the Nd and Sr isotope systems.

7.6. A petrogenetic model for the study area

Figure 8 illustrates the proposed model for the production of the magmas of the study area, in the form of trends labelled 'a' to 'e'. Mafic melts (with 49 to 57 wt% SiO_2) were produced from a range of enriched mantle compositions, along array 'a', extending from a point near EM2 to mantle that was very highly enriched by fluids evolved from the slab subducted during earlier closure of the Iapetus Ocean. This series of magmas is represented mainly by the rocks of Arrochar and Garabal Hill. Felsic magmas (70 to 77 wt% SiO_2) were

produced by partial melting of newly accreted and isotopically primitive arc crust; these plot around the dashed line 'e', which is not meant to suggest a mixing trend, but to indicate a degree of variability in the compositions of partial melts derived from the source of the felsic magmas of Glen Fyne. Mixing between various mantle melts, along 'a', and the crustal melts then produced the various main magma compositions found in the complexes (trends 'b' and 'c'). Most of the Glen Fyne enclave magmas seem to have been produced by mixing between a magma derived from the enriched mantle (similar to EM1 melt) and the crustally derived, felsic, Glen Fyne host magmas (trends 'd'). The enclave parent magma/s evidently played no part in production of the magmas of the main series, having simply been hybridised to varying degrees, mainly by diffusive processes, as a function of their residence time in contact with their host magmas.

10. Conclusions

The high-K Arrochar and Garabal Hill-Glen Fyne magmas had strong mantle connexions. Multi-element plots and initial Sr isotope ratios also indicate the presence of a crustal component. However, the isotope data show that none of the Arrochar and Glen Fyne magmas could have been produced solely by partial melting of any of the candidate crustal basement materials in the region. Bulk assimilation of candidate lower and upper crustal rocks by mantle-derived magma cannot simultaneously satisfy the constraints from the data on isotope ratios and elemental concentrations. Assimilation of partial melt from the various candidate crustal materials can also be discounted, as can models based on fractionation of mafic magmas to produce the felsic components of the complexes. Our data suggest that the mafic to intermediate rocks crystallised from melts that were derived through partial melting of mantle that had previously been heavily metasomatised by slab-derived fluids, during the subduction accompanying the closure of the Iapetus Ocean, some 70 Myr prior to the generation of the magmas of the study area in a postorogenic setting. The most felsic magmas

of the complexes were formed by partial melting of young crustal materials, most probably the arc crust formed during the previous subduction epoch. The rest of the voluminous magmas of the study area represent mixtures between the highly enriched mantle melts and the felsic crustal melts. Since there are no signs of this mixing at the present level of exposure, we infer that the mixing processes took place deeper in the crust, in some sort of magma storage area, which could correspond to a MASH (Melting Assimilation Storage and Homogenisation) zone (Hildreth and Moorbath, 1988) or a deep crustal hot zone (Annen et al., 2006). The magmatic enclaves present in some of the felsic rocks of the area were not formed from either of the two main magmas mentioned above. They represent accessory magmas produced by partial melting of ordinary enriched mantle and hybridised by varying periods of residence in, and chemical and mechanical mixing with, their host magmas. The enclaves play no role in the production of the main magma series in the complexes.

One implication of the data presented here is that the potassium enrichment in high-K suites does not necessarily signify the presence of a direct crustal melt component. The high LILE contents and crust-like Sr isotopic signatures of some high-K calcalkaline magmas could simply indicate that the felsic magmas were produced by fractionation of more mafic melts that were derived from mantle that had been highly enriched by subduction-derived fluids. Major hybridisation processes that produce magma series such as that described here may commonly occur deep in the crust and their action may not be apparent through any sort of mingling or mixing process preserved in the textures of the rocks. Enclave suites commonly form elements of spectacular mingling processes that occurred near the levels at which their host granitoid magmas were emplaced. However, it should not be assumed that such enclave magmas necessarily had any significant role in the production of the chemical variations in their host magmas.

Acknowledgements

JDC and DPF are grateful to Caroline Flinders, daughter of the late Dr Jim Flinders, for providing manuscript materials upon which some of this paper is based. Manchester University loaned us some thin sections from Dr Flinders's PhD study. Paul Henney and Gus Gunn from the British Geological Survey kindly provided the DRR samples. We thank Jim Beard and an anonymous reviewer for their critical and constructive comments, which helped us to clarify our arguments and make the paper more digestible. NERC Isotope Geosciences Laboratory Publication Number IPR/109-81C.

References

- Anderson, J.G.C., 1935. The Arrochar intrusive complex. *Geological Magazine* 72, 263 – 282.
- Annen, C., Blundy, J.D., Sparks, R.S.J., 2006. The genesis of intermediate and silicic magmas in deep crustal hot zones. *Journal of Petrology* 47, 505-539.
- Appleby, S.K., Graham, C.M., Gillespie, M.R., Hinton, R.W., Oliver, G.J.H., 2006. New insights into granite genesis from isotopic and REE micro-analyses of zircons: The Scottish Caledonian granites. *Geochimica et Cosmochimica Acta*, 70, Suppl. 1, Goldschmidt Conference Abstracts, A19.
- Armstrong, H.A., Owen, A.W., 2001. Terrane evolution of the paratectonic Caledonides of northern Britain. *Journal of the Geological Society of London* 158, 475 – 486.
- Bamford, D., Nunn, K., Prodehl, C., Jacob, B., 1978. LISPB IV. Crustal structure of Northern Britain. *Journal of the Royal Astronomical Society (Geophysics)* 54, 43 – 60.
- Barbero, L., Villaseca, C., Rogers, G., Brown, P.E., 1995. Geochemical and isotopic disequilibrium in crustal melting - An insight from the anatectic granitoids from Toledo, Spain. *Journal of Geophysical Research-Solid Earth* 100(B8), 15745 – 15765.

- Bea, F., 1996. Controls on the trace element composition of crustal melts. *Transactions of the Royal Society of Edinburgh Earth Sciences* 87, 33 – 41.
- Beard, J.S., 2008. Crystal-melt separation and the development of isotopic heterogeneities in hybrid magmas. *Journal of Petrology* 49, 1027–1041.
- Beard, J.S., Bergantz, G.W., Defant, M.J., Drummond, M.S., 1993. Origin and emplacement of low-K silicic magmas in subducting setting. Penrose Conference Report. *GSA Today* 3, 38.
- Beard, J.S., Ragland, P.C., Crawford, M.L., 2005. Reactive bulk assimilation: a model for crust-mantle mixing in silicic magmas. *Geology* 33, 681-684.
- Borg, L.E., Clyne, M.A., Bullen, T.D., 1997. The variable role of slab-derived fluids in the generation of a suite of primitive calcalkaline lavas from the southernmost Cascades, California. *Canadian Mineralogist* 35, 425 – 452.
- Borg, S.G., De Paolo, D.J., Smith, B.M., 1990. Isotopic structure and tectonics of the Central Transantarctic Mountains. *Journal of Geophysical Research* 95 (B5), 6647 – 6667.
- Chambers, L., Darbyshire, F., Noble, S., Ritchie, D., 2005. NW UK continental margin: chronology and isotope geochemistry. *British Geological Survey Commissioned Report CR/05/095*.
- Chappell, B.W., White, A.J.R., 1974. Two contrasting granite types. *Pacific Geology* 8, 173 – 174.
- Chappell, B.W., White, A.J.R., 2001. Two contrasting granite types: 25 years later. *Australian Journal of Earth Science* 48, 489 – 499.
- Chauvel, C., Hofmann, A.W., Vidal, P., 1992. HIMU-EM: The French Polynesian connection. *Earth and Planetary Science Letters* 110, 99 – 119.
- Clemens, J.D., Helps, P.A., Stevens, G., 2009. Chemical structure in granitic magmas – a signal from the source? *Proceedings of the Royal Society of Edinburgh, Earth Sciences* 100, in press.

- Clemens, J.D., Watkins, J.M., 2001. The fluid regime of high-temperature metamorphism during granitoid magma genesis. *Contributions to Mineralogy and Petrology* 140, 600 – 606.
- Cliff, R.A., Rex, D.C., 1989. Evidence for a “Grenville” event in the Lewisian of the northern Outer Hebrides. *Journal of the Geological Society of London* 146, 921 – 924.
- Conceição, R.V., Mallmann, G., Koester, E., Schilling, M., Bertotto, G.W., Rodriguez-Vargas, A., 2005. Andean subduction-related mantle xenoliths: Isotopic evidence of Sr–Nd decoupling during metasomatism. *Lithos* 82, 273-287.
- Davies, G.R., Tommasini, S., 2000. Isotopic disequilibrium during rapid crustal anatexis: implications for petrogenetic studies of magmatic processes. *Chemical Geology* 162, 169 – 191.
- Davis, J., Hawkesworth, C., 1993. The petrogenesis of 30-20 Ma basic and intermediate volcanics from the Mogollon-Datil Volcanic Field, New-Mexico, USA. *Contributions to Mineralogy and Petrology* 115, 165 – 183.
- DePaolo, D.J., Linn, A.M., Schubert, G., 1991. The continental crustal age distribution: methods of determining mantle separation ages from Sm-Nd isotopic data and application to the Southwestern United States. *Journal of Geophysical Research* 96 (B2), 2071 – 2088.
- Dickin, A.P., Bowes, D.R., 1991. Isotopic evidence for the extent of early Proterozoic basement in Scotland and north-west Ireland. *Geological Magazine* 128, 385 – 388.
- Elliott, T., Plank, T., Zindler, A., White, W., Bourdon, B., 1997. Element transport from slab to volcanic front at the Mariana arc. *Journal of Geophysical Research* B102, 14991 – 15019.
- Elliott, T., Thomas, A., Jeffcote, A., Niu, Y., 2006. Lithium isotope evidence for subduction-enriched mantle in the source of mid-ocean-ridge basalts. *Nature* 443, 565 – 568.
- Evans, J.A., 1999. Sm-Nd and U-Pb provenance traversing of the Dalradian of Scotland.

- Iterim report NERC Isotope Geosciences Laboratory Project 40124.
- Ferrando, S., Frezzotti, M.L., Dalli, L., Compagnoni, R., 2005. Multiphase solid inclusions in UHP rocks (Su-Lu, China): remnants of supercritical silicate-rich aqueous fluids released during continental subduction. *Chemical Geology* 223, 68 – 81.
- Flinders, J., 1995. A study of the Arrochar-Garabal Hill and Glen Fyne intrusions, south-west Grampians, Scotland. Ph.D. Thesis (Unpublished), Manchester University.
- Flinders, J., Clemens, J. D., 1996. Non-linear dynamics, chaos, complexity and enclaves in granitoid magmas. *Transactions of the Royal Society of Edinburgh Earth Sciences* 87, 217 – 223.
- Friend, C.R.L., Kinny, P.D., 1995. New evidence for protolith ages of Lewisian granulites northwest Scotland. *Geology* 23, 1027 – 1030.
- Friend, C.R.L., Kinny, P.D., 2001. A reappraisal of the Lewisian Gneiss Complex: geochronological evidence for tectonic assembly of disparate terranes in the Proterozoic. *Contributions to Mineralogy and Petrology* 142, 198 – 218.
- Frost, B.R., Barnes, C.G., Collins, W.J., Arculus, R.J., Ellis, D.J., Frost, C.D., 2001. A geochemical classification for granitic rocks. *Journal of Petrology* 42, 2033 – 2048.
- Frost, C.D., O’Nions, R.K., 1985. Caledonian magma genesis and crustal recycling. *Journal of Petrology* 26, 515 – 544.
- Gill, J.B., 1981. *Orogenic Andesites and Plate Tectonics*. Springer, Berlin. 390 pp.
- Glazner, A.F., 2007. Thermal limitations on incorporation of wall rock into magma. *Geology* 35, 319 – 322.
- Halliday, A.N., 1984. Coupled Sm-Nd and U-Pb systematics in late Caledonian granites and the basement under northern Britain. *Nature* 307, 229 – 233.
- Halliday, A.N., Stephens, W.E., Hunter, R.H., Menzies, M.A., Dickin, A.P., Hamilton, P.J., 1985. Isotopic and chemical constraints on the building of the deep Scottish lithosphere. *Scottish Journal of Geology* 21, 465 – 491.

- Harmon, R.S., Halliday, A.N., 1980. Oxygen and strontium isotope relationships in the British late-Caledonian granites. *Nature* 283, 21 – 25.
- Harper, C.J., 1967. The geological interpretation of potassium-argon ages of metamorphic rocks of the Scottish Caledonides. *Scottish Journal of Geology* 3, 46 – 66.
- Hildreth, W., Moorbath, S., 1988. Crustal contributions to arc magmatism in the Andes of Central Chile. *Contributions to Mineralogy and Petrology* 98, 455–489.
- Ishikawa, T., Fujisawa, S., Nagaishi, K., Masuda, T., 2005. Trace element characteristics of the fluid liberated from amphibolite-facies slab: Inference from the metamorphic sole beneath the Oman ophiolite and implication for boninite genesis. *Earth and Planetary Science Letters* 240, 355 – 377.
- Janák, M., Petrik, I., Poller, U., 2001. Disequilibrium melting in Early Devonian (406 Ma) orthogneisses from the Western Tatra Mts. *Geolines* 13, 66 – 67.
- Johnston, G.S., Wright, J.E., 1957. The geology of the tunnels of the Loch Sloy hydro-electric scheme. *Geological Survey Bulletin* 12, 1 – 17.
- Kelemen, P.B., Yogodzinski, G.M., Scholl, D.W., 2004. Along-strike variation in lavas of the Aleutian island arc: implications for the genesis of high Mg# andesite and the continental crust. In: J. Eiler (Editor), *Inside the Subduction Factory*. American Geophysical Union.
- Kessel, R., Schmidt, M.W., Ulmer, P., Pettke, T., 2005. Trace element signature of subduction-zone fluids, melts and supercritical liquids at 120 – 180 km depth. *Nature* 437, 724 – 727.
- Killian, R., Stern, C.R., 2002. Constraints on the interaction between slab melts and the mantle wedge from adakitic glass in peridotite xenoliths. *European Journal of Mineralogy* 14, 25 – 36.

- Kinny, P.D., Friend, C.R.L., 1997. U-Pb isotopic evidence for the accretion of different crustal blocks to form the Lewisian Complex of north-west Scotland. *Contributions to Mineralogy and Petrology* 129, 326 – 340.
- Kinny, P.D., Friend, C.R.L., 2005. Proposal for a terrane-based nomenclature for the Lewisian Gneiss Complex of NW Scotland. *Journal of the Geological Society of London* 162, 175 – 186.
- Kushiro, I., 1990. Partial melting of mantle wedge and evolution of island arc crust. *Journal of Geophysical Research* 95, 15929 – 15939.
- Larsen, L.M., Pedersen, A.K., Sundvoll, B., Frei, R., 2003. Alkali picrites formed by melting of old metasomatized lithospheric mantle: Manitdlat Member, Vaigat Formation, Palaeocene of West Greenland. *Journal of Petrology* 44, 3 – 38.
- Le Maitre, R.W., Bateman, P., Dudek, A., Keller, J., Lameyre Le Bas, M.J., Sabine, P.A., Schmid, R., Sorensen, H., Streckeisen, A., Wolley, A.R., Zanettin, B., 1989. *A Classification of Igneous Rocks and Glossary of Terms*. Blackwell, Oxford.
- Lyon, T.D.B., Bowes, D.R., 1977. Rb-Sr U-Pb and K-Ar isotopic study of the Lewisian complex between Durness and Loch Laxford Scotland. *Krystalinikum* 13, 53 – 72.
- Marcantonio, F., Dickin, A. P., McNutt, R.H., Heaman, L.M., 1988. A 1,800-million-year-old Proterozoic gneiss terrane in Islay with implications for the crustal structure and evolution of Britain. *Nature* 335, 62 – 64.
- McDonough, W.F., Sun, S-S., 1995. Composition of the Earth. *Chemical Geology* 120, 223 – 253.
- Menzies, M.A., Halliday, A., 1988. Lithospheric domains beneath the Archaean and Proterozoic crust of Scotland. *Journal of Petrology Special Lithosphere Issue*, 275 – 302.
- Middlemost, E.A.K., 1994. Naming materials in the magma igneous rock system. *Earth Science Reviews* 37, 215 – 224.

- Morton, A.C., Taylor, P.N., 1991. Geochemical and isotopic constraints on the nature and age of basement rocks from Rockall Bank, NE Atlantic. *Journal of the Geological Society of London* 148, 631 – 634.
- Moyen, J-F., Stevens, G., 2005. Experimental constraints on TTG petrogenesis: implications for Archean geodynamics. In: Benn, K., Mareschal, J-C. and Condie, K.C. (Editors), *Archean Geodynamics and Environments*, pp. 149-175.
- Nockolds, S.R., 1941. The Garabal-Hill Glen Fyne igneous complex. *Journal of the Geological Society of London* 96, 451 – 511.
- Park, R.G., Tarney, J., 1987. The Lewisian complex: a typical Precambrian high-grade terrain? In: Park, R.G., Tarney, J. (Eds), *Evolution of the Lewisian and Comparable Precambrian Terrains*. Geological Society Special Publication 27, 13 – 25.
- Patiño Douce, A.E., 1995. Experimental generation of hybrid silicic melts by reaction of high-Al basalt with metamorphic rocks. *Journal of Geophysical Research* 100(B8), 15623 – 15639.
- Pidgeon, R.T., Aftalion, M., 1978. Cogenetic and inherited zircon U-Pb systems in granites: Palaeozoic granites of Scotland and England. *Crustal Evolution in north-western Britain and adjacent regions*. Geological Journal Special Issue 10, 183 – 220.
- Plank, T., Langmuir, C.H., 1993. Tracing trace elements from sediment input to volcanic output at subduction zones. *Nature* 362, 739 – 742.
- Plank, T., Langmuir, C.H., 1998. The geochemical composition of subducting sediment and its consequences for the crust and mantle. *Chemical Geology* 145, 325 – 394.
- Portnyagin, M., Hoernle, K., Plechov, P., Mironov, N., Khubunaya, S., 2007. Constraints on mantle melting and composition and nature of slab components in volcanic arcs from volatiles (H₂O, S, Cl, F) and trace elements in melt inclusions from the Kamchatka Arc. *Earth and Planetary Science Letters* 255, 53–69.

- Rapp, R.P., Shimizu, N., Norman, M.D., Applegate, G.S., 1999. Reaction between slab-derived melts and peridotite in the mantle wedge: experimental constraints at 3.8 GPa. *Chemical Geology* 160, 335 – 356.
- Rehkamper, M., Hofmann, A.W., 1997. Recycled ocean crust and sediment in Indian Ocean MORB. *Earth and Planetary Science Letters* 147, 93 – 106.
- Roberts, M.P., Clemens, J.D., 1993. Origin of high-potassium, calcalkaline, I-type granitoids. *Geology* 21, 825 – 828.
- Rogers, G., Dunning, G.R., 1991. Geochronology of appinitic and related granitic magmatism in the western Highlands of Scotland: constraints on the timing of transcurrent fault movement. *Journal of the Geological Society of London* 148, 17 – 27.
- Sanders, I.S., Van Calsteren, P.W.C., Hawksworth, C.J., 1984. A Grenville Sm-Nd age for the Glenelg eclogite in north west Scotland. *Nature* 312, 439 – 440.
- Sawyer, E.W., 1991. Disequilibrium melting and the rate of melt-residuum separation during migmatization of mafic rocks from the Grenville Front, Quebec. *Journal of Petrology* 32, 701 – 738.
- Schaltegger, U., Corfu, F., 1992. The age and source of Late Hercynian magmatism in the central Alps - evidence from precise U-Pb ages and initial Hf isotopes. *Contributions to Mineralogy and Petrology* 111, 329 – 344.
- Schmidt, M.W., Vielzeuf, D., Auzanneau, E., 2004. Melting and dissolution of subducting crust at high pressures: the key role of white mica. *Earth and Planetary Science Letters* 228, 65 – 84.
- Sisson T.W., Ratajeski K., Hankins W.B., Glazner A.F., 2005. Voluminous granitic magmas from common basaltic sources. *Contributions to Mineralogy and Petrology* 148, 635 – 661.

- Spera, F.J., Bohron, W.A., 2001. Energy-constrained open system magmatic processes I: general model and energy-constrained assimilation and fractional crystallization (EC-AFC) formulation. *Journal of Petrology* 42, 999-1018.
- Steinhefel, G., Hegner, E., Oliver, G.J.H., 2008. Chemical and Nd isotope constraints on granitoid sources involved in the Caledonian Orogeny in Scotland. *Journal of the Geological Society of London* 165, 817 – 827.
- Stephens, W.E., Halliday, A.N., 1984. Geochemical constraints between late-Caledonian granitoid plutons of north, central and southern Scotland. *Transactions of the Royal Society of Edinburgh Earth Sciences* 75, 259 – 273.
- Summerhayes, C.P., 1966. A geochronological and strontium isotope study of the Garabal-Hill Glen Fyne igneous complex, Scotland. *Geological Magazine* 103, 153 – 165.
- Tatsumi, Y., Kogiso, T., 1997. Trace element transport during dehydration processes in the subducted oceanic crust: 2. Origin of chemical and physical characteristics in arc magmatism. *Earth and Planetary Science Letters* 148, 207 – 221.
- Vernon, R.H., 1990. Crystallization and hybridism in microgranitoid enclave magmas - microstructural evidence. *Journal of Geophysical Research* 95(B11), 17849-17859.
- Ventura, G., Del Gaudio, P., Iezzi, G., 2006. Enclaves provide new insights on the dynamics of magma mingling: A case study from Salina Island (Southern Tyrrhenian Sea, Italy). *Earth and Planetary Science Letters* 243, 128 – 140.
- Villaros, A., 2009. The petrogenesis of the S-type granites of the Cape Granite Suite, with emphasis on the Peninsular Pluton and Darling Batholith. PhD (unpubl.) thesis, University of Stellenbosch, South Africa.
- Villaros, A., Stevens, G., Moyon, J-F., Buick, I.S., 2009. The trace element compositions of S-type granites: Evidence for disequilibrium melting and accessory phase entrainment in the source. *Chemical Geology*, in press.

- Watt, G.R., Harley, S.L., 1993. Accessory phase controls on the geochemistry of crustal melts and restites produced during water-undersaturated partial melting. *Contributions to Mineralogy and Petrology* 114, 55 – 566.
- Whitaker, M.L., Nekvasil, H., Lindsley, D.H., McCurry, M., 2008. Can crystallization of olivine tholeiite give rise to potassic rhyolites? – an experimental investigation. *Bulletin of Volcanology* 70, 417 – 434.
- Xiong, X.L., Xia, B., Xu, J.F., Niu, H.C., Xiao, W.S., 2006. Na depletion in modern adakites via melt / rock reaction within the sub-arc mantle. *Chemical Geology* 229, 273 – 292.
- Zindler, A., Hart, S.R., 1986. Chemical Geodynamics, *Annual Review of Earth and Planetary Sciences* 14, 493 – 571.

Appendix A

Table A1

Conversion from sample locations on Figures 3 and 4 to sample numbers used in the rest of the paper and Flinders (1995)

number on map	sample number	rock type	number on map	sample number	rock type
1	ARR 09.89/20	granodiorite	12	GF 12.89/2	granite
2	ARR 04.90/5	monzodiorite	13	DRR 129.2	monzodiorite
3	ARR 04.90/3	gabbro	14	DRR 130*	ultramafic rock
4	ARR 09.89/11	diorite	15	DRR 132	ultramafic rock
5	GF 10.90/15	granodiorite	16	GF 02.92/24	granite
6	GF 10.90/16	quartz monzonite	17	GF 10.90/10	granite
7	GF 06.91/9	quartz monzonite	18	GF 07.91/5	Dalradian schist
8	GF 10.90/5	granite	19	GH 04.90/20	granodiorite
9	GF 10.90/14	quartz monzonite	20	GF 10.89/6	monzonite
10	GF 06.91/7F	granodiorite	21	GF 02.92/23	monzonite
11	GF 06.91/4A	quartz monzonite			

* sample analysed but subsequently found to be completely serpentinised and therefore not included in the analytical dataset presented in Tables 1 and 2

Appendix B

Table B1

Analysed host rocks and their enclaves*

host	enclaves
ARR 04.90/5	ARR 04.90/5
GF04.90/14	GF04.90/16B, GF04.90/16C
GF10.90/5	GF10.90/5
GF10.90/15	GF10.90/15
GF10.90/16	GF12.89/12B
GF06.91/4A	GF10.89/5B, GF10.89/5H
GF06.91/7F	GF06.91/7B, GF06.91/7C, GF06.91/7D, GF06.91/7E, GF06.91/7F
GH04.90/20	GH04.90/18

* see Tables 1 and 2 for the analytical data

Appendix C

Whole-rock analytical techniques

Major- and trace-element analytical methods

The analyses were carried out by XRF, using pressed powder pellets, at the University of Manchester. Fifteen standard reference materials were used and the calibration data were fitted with quadratic equations. Standard relative errors for the major oxides are: $\text{SiO}_2 \pm 1\%$, Al_2O_3 , FeO , MgO and $\text{CaO} \pm 3\%$ (for values > 5 wt%), MnO and $\text{P}_2\text{O}_5 \pm 10\%$, other oxides in concentrations of 3 to 5 wt% $\pm 5\%$, and other oxides in concentrations of 1 to 2 wt% $\pm 10\%$. For the trace elements, detection limits were all around 5 ppm; maximum errors are: for elements in concentrations ≥ 50 ppm $\pm 10\%$, for elements in concentrations between 10 and 50 ppm $\pm 20\%$, and for elements in concentrations < 10 ppm $\pm 40\%$. Reproducibility was checked by carrying out a duplicate analysis in each analytical session. Major-oxide analyses were reproducible to ~ 1 rel.% and trace elements to between 1 and 5 rel.%.

Isotope analytical methods

The isotope analyses were carried out at the NERC Isotope Geosciences Laboratory at Keyworth, UK. Concentrations of rubidium (Rb) and strontium (Sr) and the Rb/Sr atomic ratios were determined by XRF spectrometry at the British Geological Survey. Samples for Sm-Nd analysis were spiked with ^{150}Nd - and ^{147}Sm -enriched tracers and decomposed using a mixture of HF and HNO_3 acids in sealed Savillex[®] bombs at 120 °C. Following treatment with HNO_3 and conversion to chlorides, with 6 M HCl, Sr and the rare-earth elements (REE) were separated by ion exchange, using Biorad[®] AG50W-X8 resin. Sm and Nd were separated from the REE fraction by reversed-phase ion exchange chromatography on a column filled with Biobeads[®] coated with di-2-ethylhexyl orthophosphoric acid. Procedural blanks were of the order of a few hundred picogrammes for Sr and a hundred picogrammes for Nd.

Isotope ratio measurements were made on an automated Finnegan-MAT 262 mass spectrometer. Errors are quoted as 2σ from the measured or calculated values. Analytical uncertainties are estimated to be $\pm 0.01\%$ for $^{87}\text{Sr}/^{86}\text{Sr}$ and $^{143}\text{Nd}/^{144}\text{Nd}$ and $\pm 1.0\%$ for both $^{87}\text{Rb}/^{86}\text{Sr}$ and $^{147}\text{Sm}/^{144}\text{Nd}$. Measured $^{143}\text{Nd}/^{144}\text{Nd}$ ratios were corrected for mass fractionation relative to $^{146}\text{Nd}/^{144}\text{Nd} = 0.7219$ and $^{87}\text{Sr}/^{86}\text{Sr}$ ratios relative to $^{86}\text{Sr}/^{88}\text{Sr} = 0.1194$. Replicate analyses of the Johnson and Matthey Nd standard, made during the period of this study, yielded 0.511149 ± 0.000027 for $^{143}\text{Nd}/^{144}\text{Nd}$. However, measured $^{143}\text{Nd}/^{144}\text{Nd}$ ratios were normalised to a value of 0.511124, equivalent to a value of 0.511861 for the La Jolla International isotope standard. The average value of $^{87}\text{Sr}/^{86}\text{Sr}$, determined for the NBS 987 strontium isotope standard, was 0.710246 ± 0.000028 ($n = 32$).

Analytical data are presented in Table 2. The corresponding calculated values for ϵNd and $^{87}\text{Sr}/^{86}\text{Sr}_{425}$ are also shown, together with Nd depleted mantle model ages (T_{DM}). The latter were calculated using to a two-stage model (see Borg et al., 1990; DePaolo et al., 1991). The value of ϵNd was calculated relative to a chondritic reservoir with $^{143}\text{Nd}/^{144}\text{Nd} = 0.512638$ and $^{147}\text{Sm}/^{144}\text{Nd} = 0.1967$.

Figure Captions

Fig. 1. Map showing the location of the study area in the Scottish Highlands. The area of the labelled rectangle is enlarged in Fig. 2.

Fig. 2. Map showing the locations of the Garabal Hill-Glen Fyne and Arrochar complexes, with respect to major geographical features. The outlined areas are enlarged in Figures 3 and 4, and show the local geology.

Fig. 3. Geological map of the Arrochar area, showing the locations of samples analysed for their Sr and Nd isotope geochemistry. The coordinate system is the British Ordnance Survey National Grid, the prefix letters being NN. The samples are numbered 1 to 4, for clarity, and the key for conversion to actual sample numbers is given in Appendix A, Table A1.

Fig. 4. Geological map of the Garabal Hill-Glen Fyne complex, showing the locations of samples analysed for their Sr and Nd isotope geochemistry. The coordinate system is the British Ordnance Survey National Grid, the prefix letters being NN. The samples are numbered 5 to 21, for clarity, and the key for conversion to actual sample numbers is given in Appendix A, Table A1.

Fig. 5. (a) $\text{SiO}_2\text{-K}_2\text{O}$ plot for the Glen Fyne rocks (large grey squares) and their enclaves (small grey squares), showing the fields for low-, medium- and high-K and shoshonite series, as defined by Le Maitre et al. (1989); (b) plot of modified lime-alkali index (MALI) against SiO_2 , showing the various chemical magma types defined by Frost et al. (2001) and points for the Arrochar and Garabal Hill-Glen Fyne rocks. Black squares – Arrochar complex, dark grey squares – Ardlui diorite, pale grey squares – Glen Fyne, white squares – Garabal Hill. In this, and all subsequent geochemical diagrams, samples are plotted on a volatile-free basis (i.e., normalised to 100%, volatile-free).

Fig. 6. Primitive mantle-normalised multi-element plots for rocks belonging to (a) Glen Fyne, with granite GF 02.92/24 plotted as a dashed line, (b) Garabal Hill, (c) Arrochar – solid lines and the Ardlui gabbro – dashed line, (d) enclaves from the various intrusions (solid lines – Glen Fyne, long dashes – Garabal Hill, short dashes – Arrochar. Normalising values are from McDonough and Sun (1995).

Fig. 7. Harker plots showing examples of the geochemical variations among the rocks from the study area. (a) Al_2O_3 , (b) CaO , (c) MgO , (d) Sr . Symbols are as in Figure 5.

Fig. 8. $^{87}\text{Sr}/^{86}\text{Sr}$ (at 425 Ma) plotted against SiO_2 content, for rocks of the study area, plus GLOSS (GLOBAL Subducting Sediment; Plank and Langmuir, 1998), country rock schist and the assumed point for a melt formed from the country rock schist. Symbols are as in Figure 5 except that enclaves are also plotted, as small squares of the same shade as their host rocks. Points for enriched mantle EM1 and EM2 melts (Zindler and Hart, 1986; Chauvel et al., 1992) are also plotted, along with a point for a magnesian Greenland alkali basalt (GAB; Larsen et al., 2003). The significance of these points is discussed in the text, along with the inferred trends (labelled 'a' to 'e').

Fig. 9. Isotope correlation diagrams, with ϵNd plotted against $^{87}\text{Sr}/^{86}\text{Sr}$ (at 425 Ma) for the rocks from the study area. The ϵNd value for bulk Earth (0) is shown as a horizontal line. In a., the additional points plotted are depleted mantle DM, enriched mantle EM1 and EM2, average continental alkali basalt (AB), country rock schist and GLOSS. See text and captions to Fig. 5 for further explanation. In b. areas are drawn to show the ranges of $^{87}\text{Sr}/^{86}\text{Sr}_{425}$ and ϵNd_{425} in candidate basement materials – the Dalradian, the Rhinnian and the Lewisian TTG rocks.

Fig. 10. Examples of refractory major oxides (a. FeO^*+MgO ; b. CaO) plotted as a function of $^{87}\text{Sr}/^{86}\text{Sr}$ at 425 Ma, for the rocks of the study area. The symbols and additional points are as in Figs 7 and 8. The equivalents of the variation trends ‘a’ to ‘e’, identified in Figure 8, are evident here. See text for discussion.

Fig. 11. Plot of ϵNd (at 425 Ma) against SiO_2 content for rocks of the study area. The ϵNd value for bulk Earth (0) is shown as a horizontal line. Symbols as in Figure 5.

Fig. 1

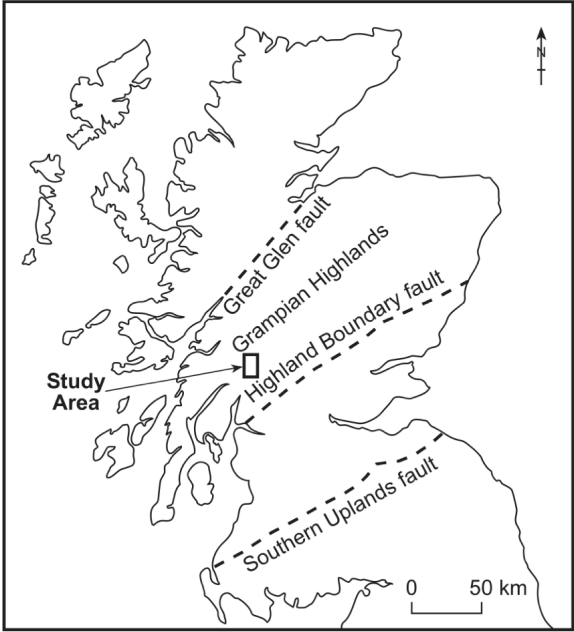


Fig. 2

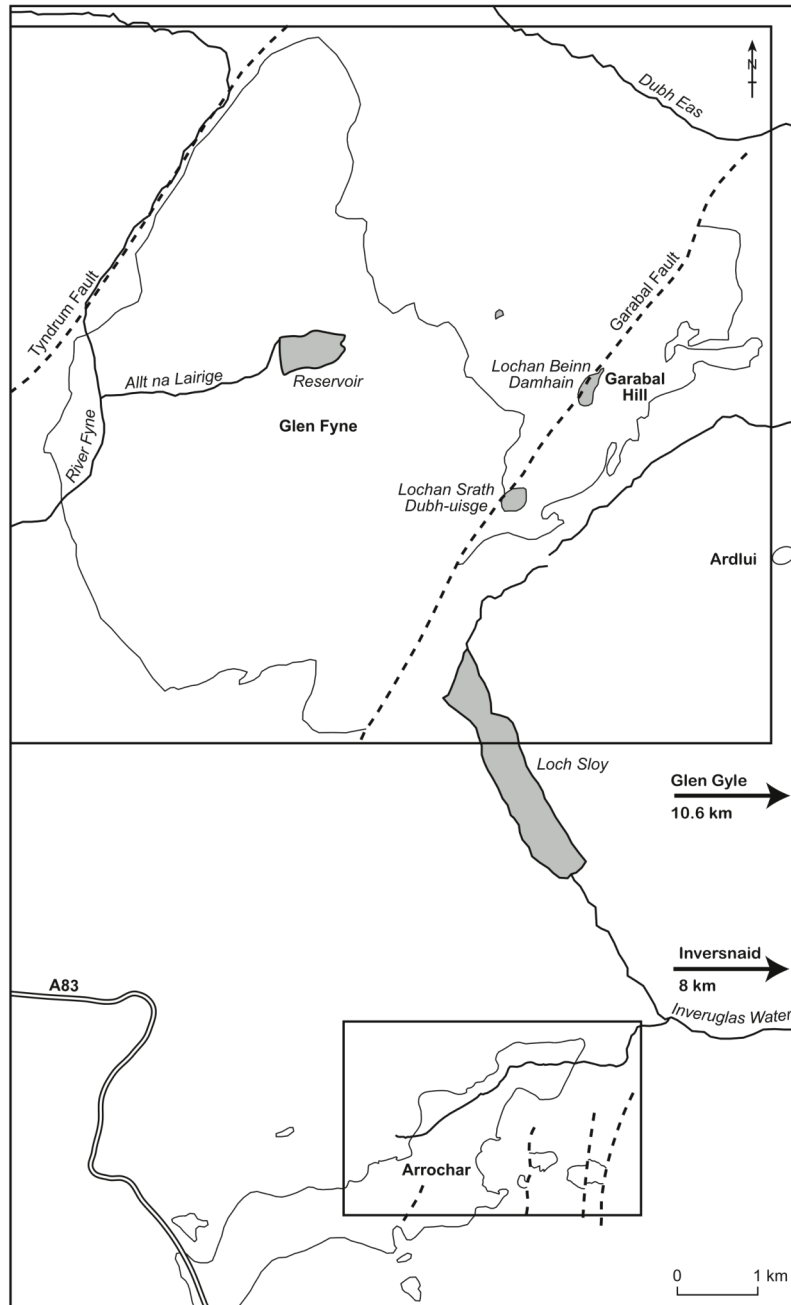


Fig. 3

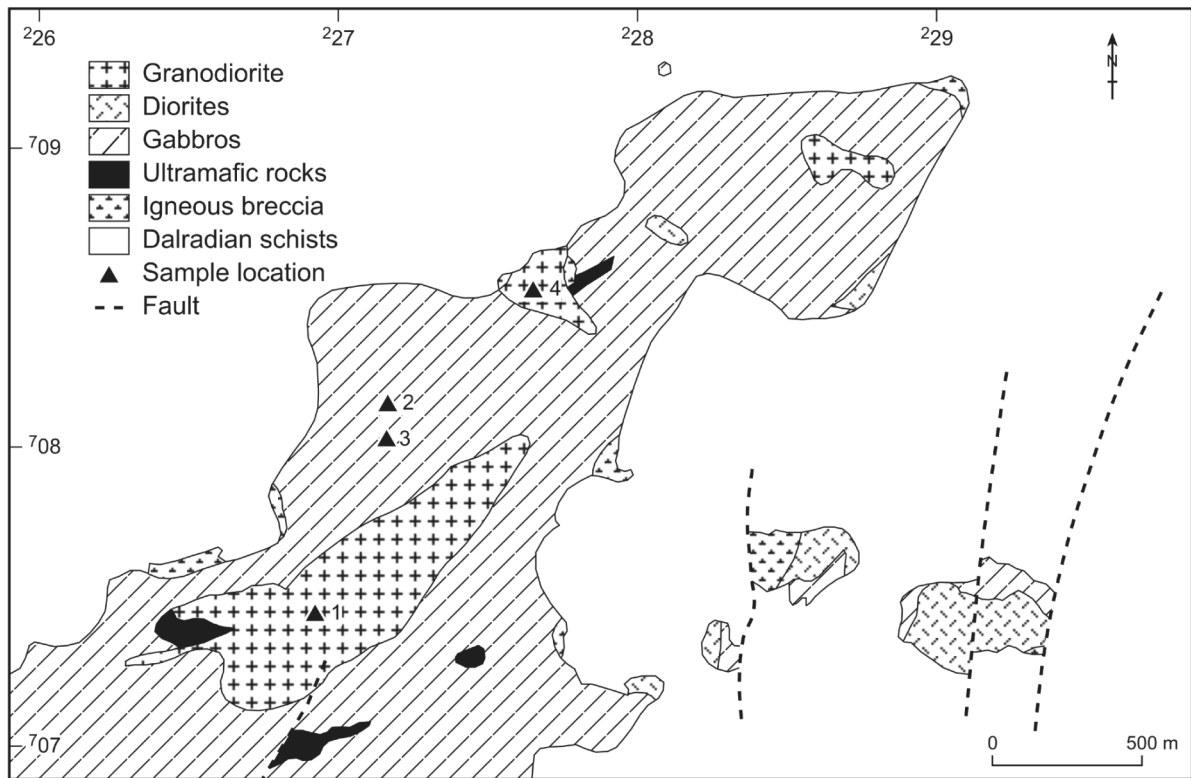


Fig. 4

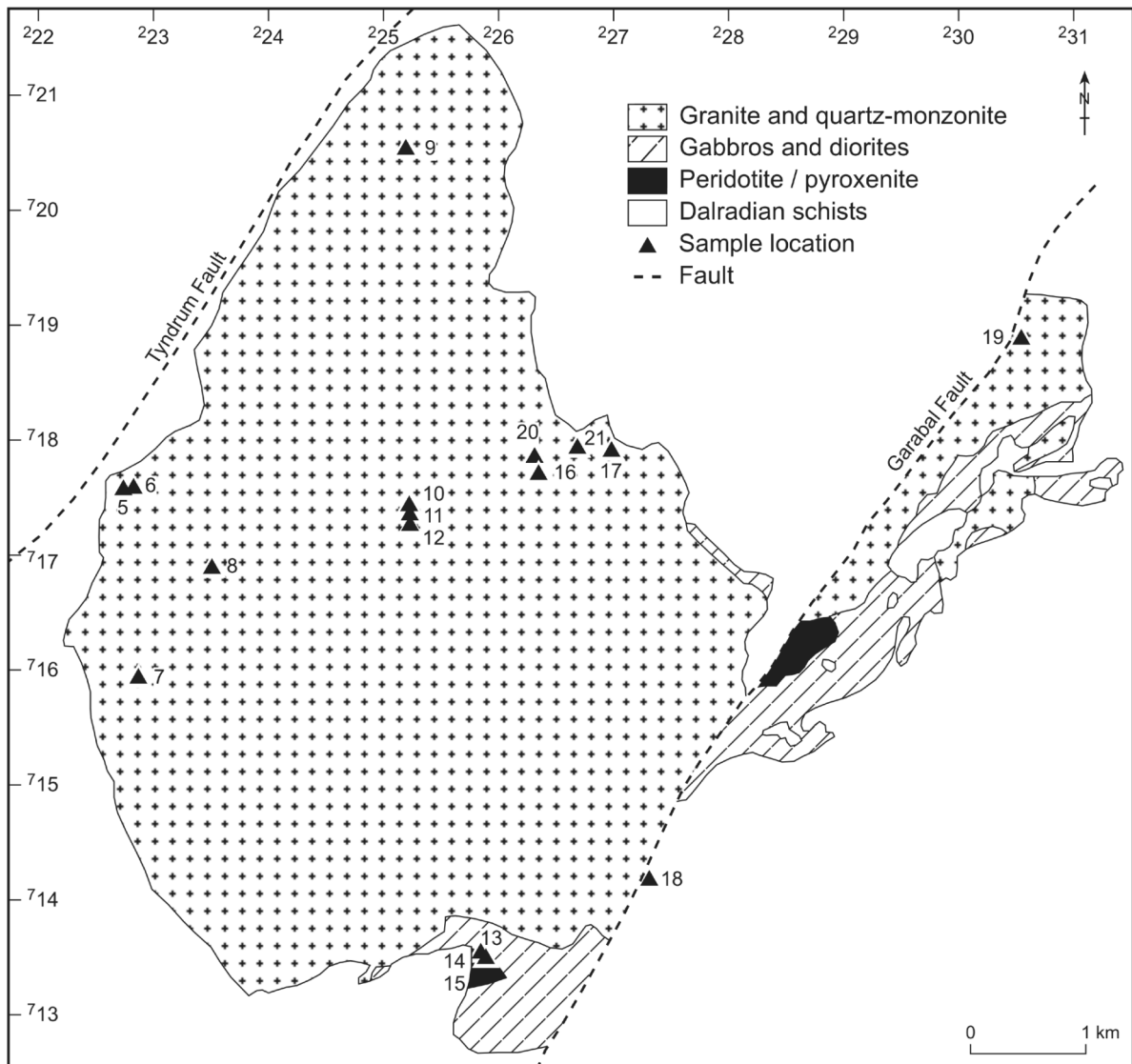


Fig. 5

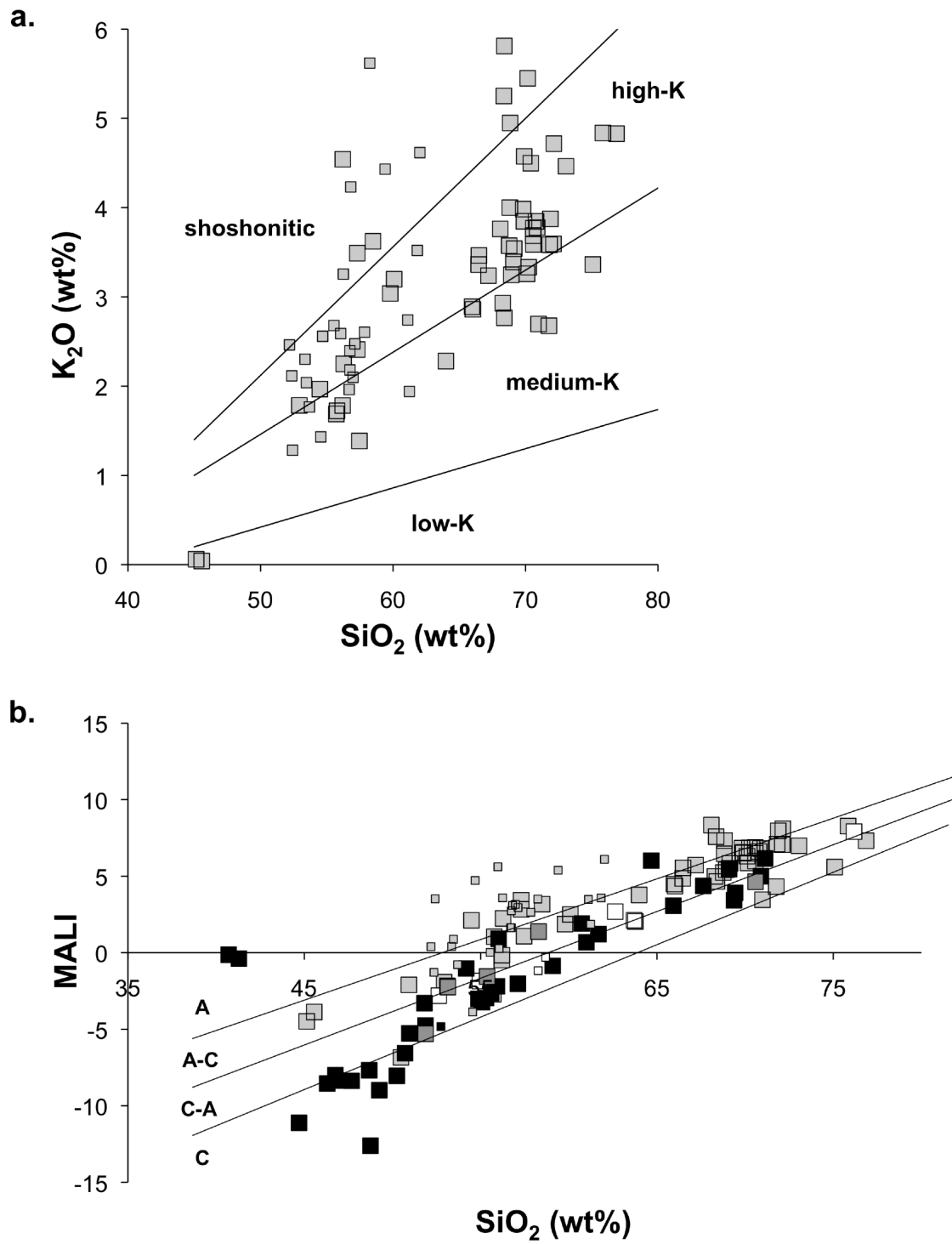


Fig. 6

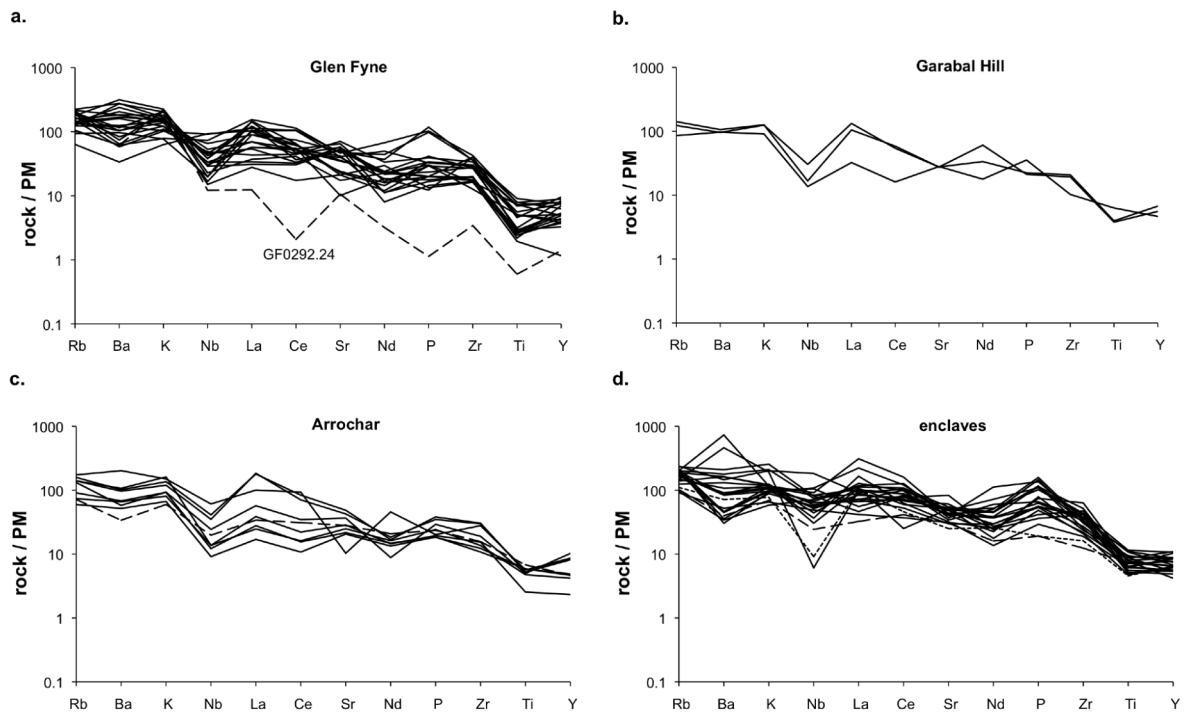


Fig. 7

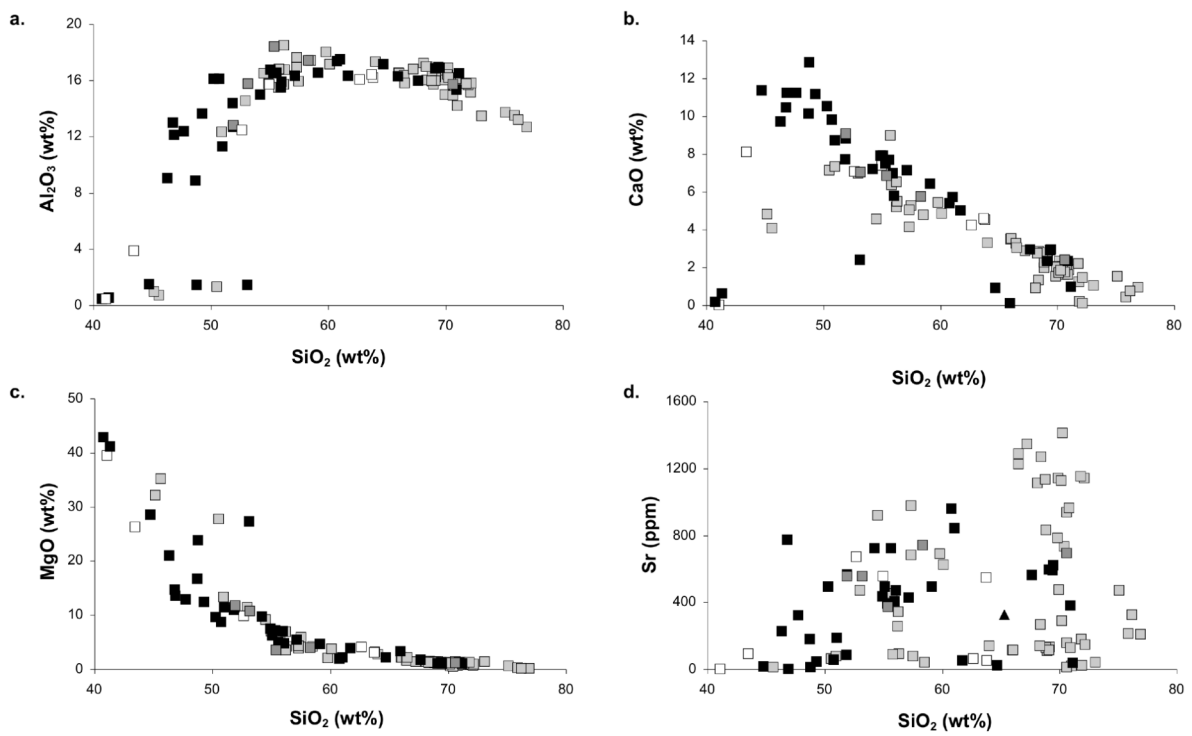


Fig. 8

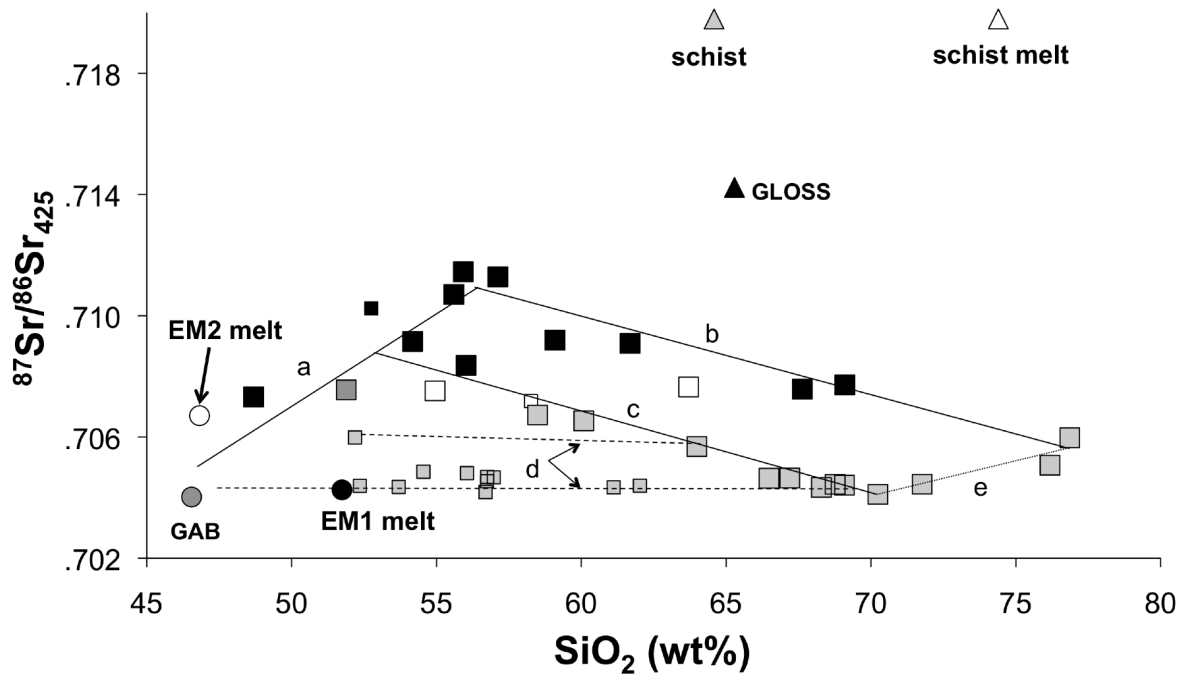


Fig. 9

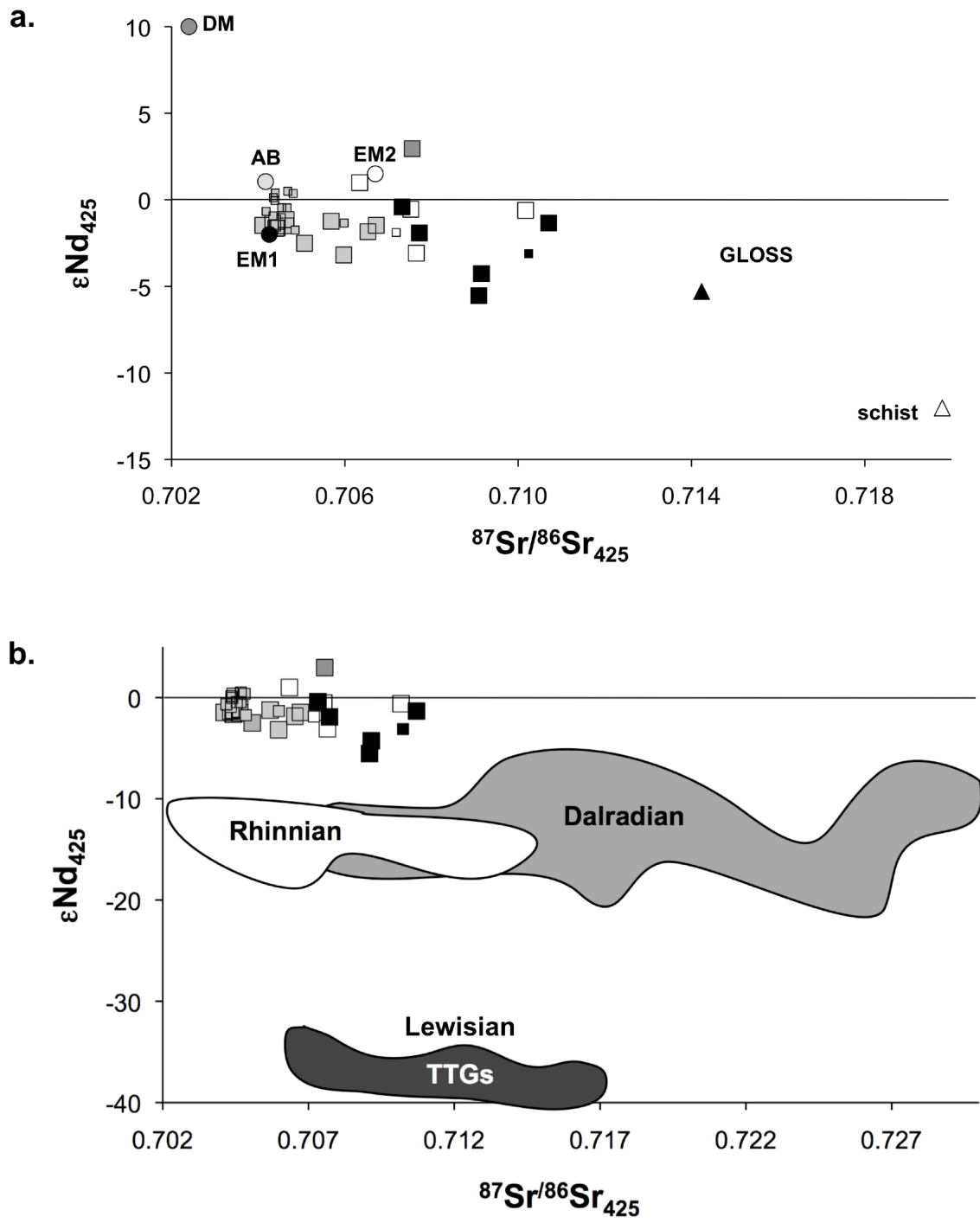


Fig. 10

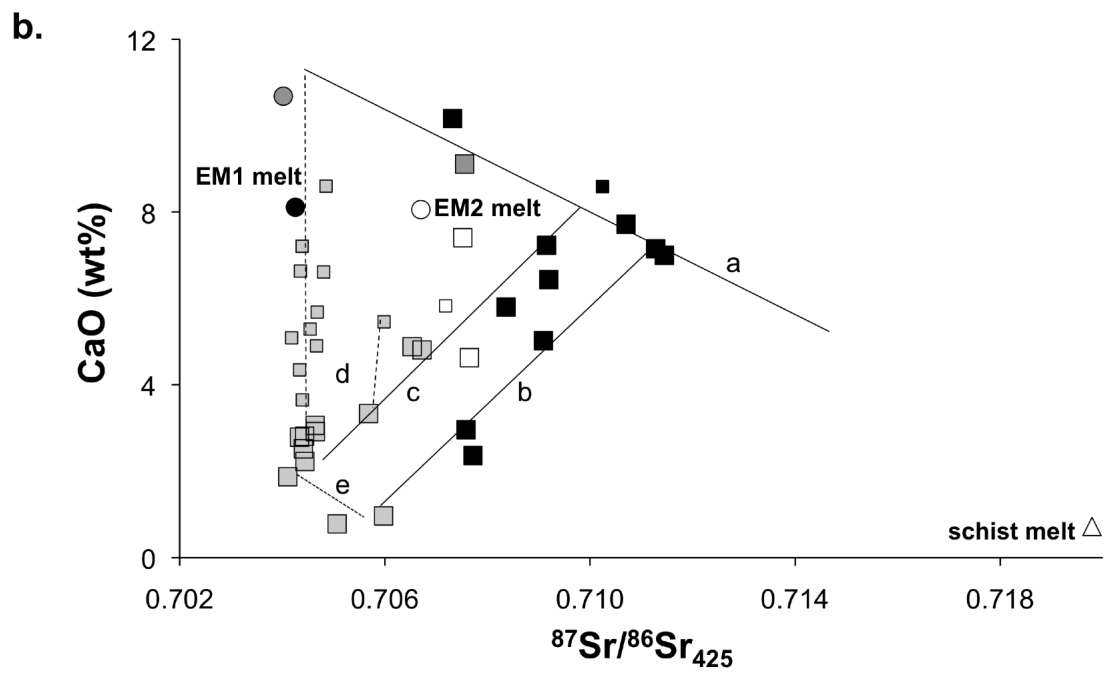
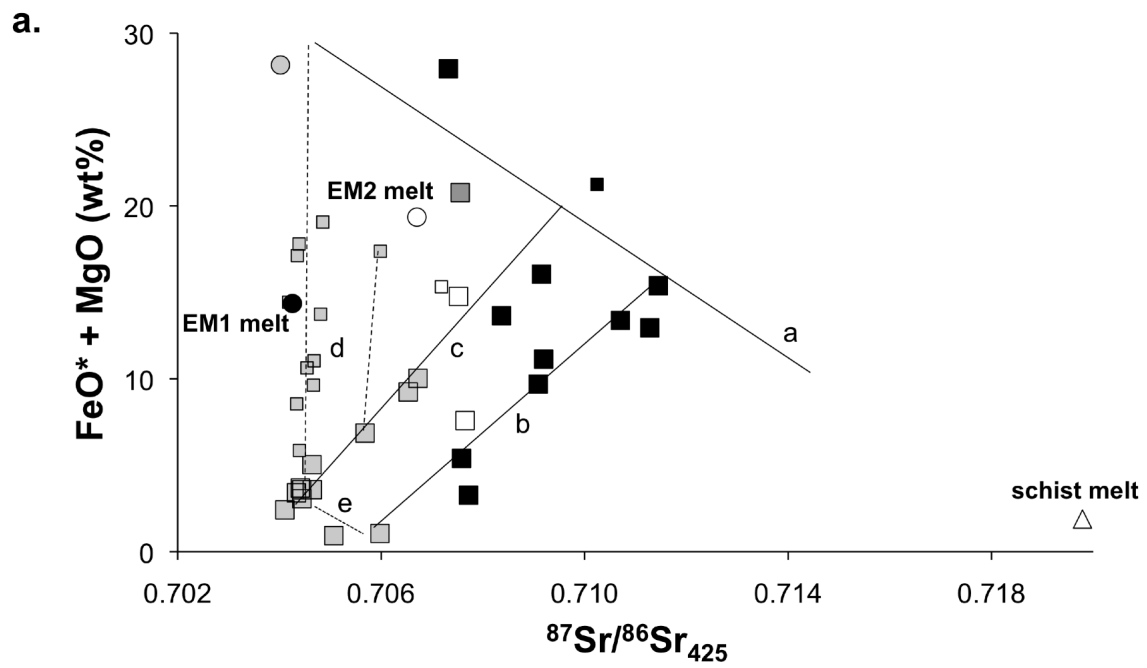


Fig. 11

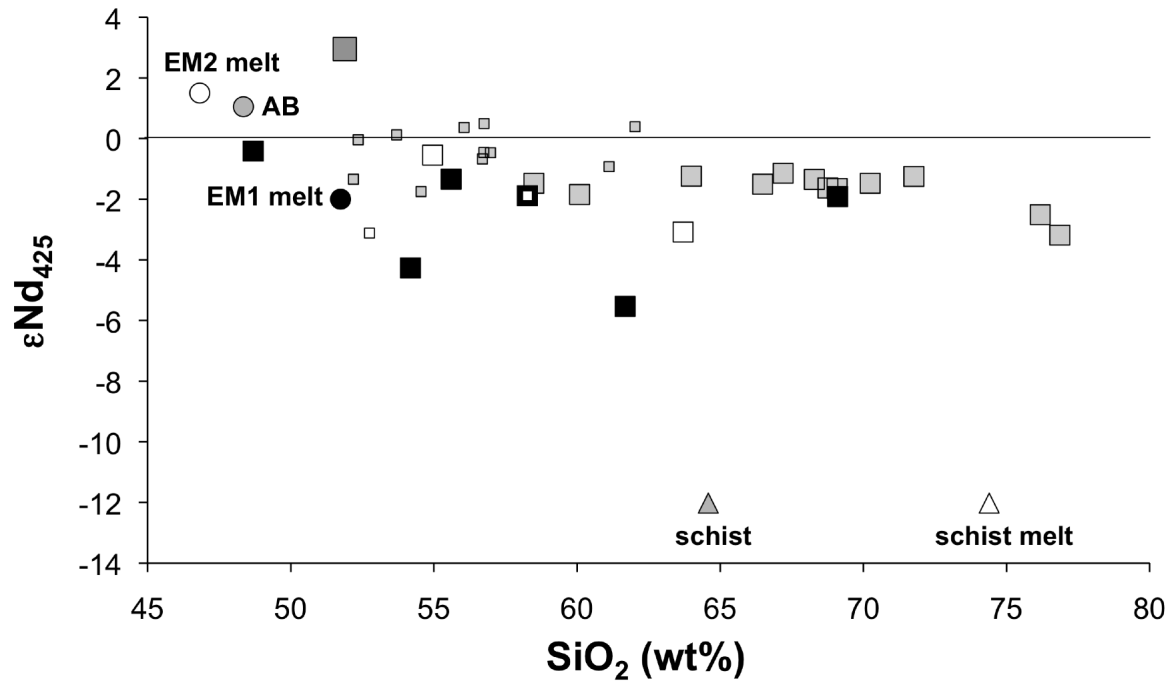


Table 1
Major- and trace-element analytical data

sample	comment	grid reference	rock name	series	SiO ₂	TiO ₂	Al ₂ O ₃	FeO*	MnO	MgO	CaO	Na ₂ O	K ₂ O	P ₂ O ₅	XRF total	Nb	Zr	Y	Sr	Rb	Zn	Cu	Ni	Cr	Ce	Nd	V	La	Ba	Sc	
Glen Fyne																															
GF 10.89/4	host			medium-K	68.40	0.51	16.99	1.88	0.03	1.52	2.88	4.77	2.77	0.25	99.80	170	203	18	1273	75	24		40	21	97		109	18	1162	4	
GF 10.89/6		22625 71775	monzonite	high-K	60.09	0.88	17.17	5.36	0.09	3.88	4.88	4.19	3.20	0.27	99.14	333	33	627	107	69	84	75	99	69		129	32	656	18		
GF 10.89/7				medium-K	75.08	0.25	13.76	1.40	0.04	0.70	1.54	3.77	3.36	0.10	99.93	255	19	475	80	32	12	23	18	34		32	29	812	3		
GF 10.89/8		2266 7178		shoshonite	68.36	0.56	16.06	3.30	0.04	1.22	1.36	3.68	5.25	0.16	99.60	19	216	33	268	150	35		49	62	57		65	31	899	7	
GF 10.89/10				medium-K	70.98	0.77	14.25	5.15	0.06	1.39	1.91	2.68	2.70	0.11	99.39	22	419	41	201	100	74		55	95	92	23	82	37	552	11	
GF 12.89/1				medium-K	70.57	0.33	16.21	1.61	0.05	0.94	1.63	4.83	3.69	0.13	99.81	19	175	5	1062	134	31		30	16	51	10	33	20	1825	7	
GF 12.89/2		2252 7172	granite	medium-K	70.24	0.35	16.21	1.22	0.05	1.19	1.87	5.39	3.33	0.14	99.93	17	181	8	1415	125	30		33	19	45		32	28	1807	5	
GF 12.89/3				medium-K	71.81	0.29	15.83	1.38	0.05	0.92	1.25	4.76	3.58	0.12	99.90	23	170	9	1082	113	25		31	14	57		26	23	1576	15	
GF 12.89/4				medium-K	70.58	0.35	15.74	1.73	0.05	1.05	2.18	4.58	3.59	0.15	99.77	358	968	24	939	86	36		31	19	45	13	39	37	1149	7	
GF 12.89/5				shoshonite	70.16	0.31	16.91	1.24	0.04	0.67	2.35	2.77	5.45	0.10	99.65	337	939	22	291	181	20		32	17	49		31	29	1234	6	
GF 12.89/7				high-K	70.79	0.31	16.06	1.43	0.05	0.81	1.91	4.67	3.85	0.12	99.83	12	210	22	966	87	34		6	26	21	64		29	32	1603	2
GF 12.89/8				medium-K	70.88	0.30	16.13	1.47	0.05	0.94	1.65	4.69	3.78	0.12	99.84	15	207	22	1031	77	37		28	16	52		31	30	1526	2	
GF 12.89/9				high-K	69.88	0.33	16.32	1.55	0.05	1.11	2.05	4.72	3.85	0.14	99.82	12	206	18	1143	80	36		29		54		31	32	1941	1	
GF 12.89/10		2239 7170		high-K	70.39	0.31	16.24	1.36	0.05	0.58	2.05	4.41	4.50	0.11	99.84	12	188	22	735	99	33		24	10	44		29	21	2133	3	
GF 12.89/11	host	2228 7160		medium-K	65.96	0.60	16.57	2.85	0.04	2.20	3.51	5.11	2.89	0.27	99.66	173	208	17	1107	69	25		63	44	84		129		828	7	
GF 12.89/11A	host			medium-K	66.03	0.61	16.52	2.85	0.04	2.24	3.54	5.04	2.86	0.27	99.64	169	216	20	1106	67	25		66	52	84		132		827	2	
GF 04.90/2				medium-K	52.93	1.03	14.58	7.54	0.13	11.51	6.99	3.28	1.78	0.23	99.19	144	31	474	76	72		10	166	490	62		223	83	407	36	
GF 04.90/3A					45.57	0.27	0.73	13.67	0.18	35.25	4.10	0.18	0.04	0.01	97.60	24	16	16													
GF 04.90/3B				medium-K	55.72	0.95	15.52	6.12	0.12	5.98	9.00	4.60	1.69	0.30	98.93	13	298	32	457	56	119		100	190	105	18	149	68	640	24	
GF 04.90/4					45.14	0.53	0.99	15.68	0.26	32.19	4.83	0.28	0.06	0.03	98.78	30	15						120	14	907	279	22	219	64	40	
GF 04.90/5				high-K	73.05	0.41	13.48	2.31	0.03	1.47	1.06	3.59	4.46	0.12	99.69	13	171	17	420	75	44		47	65	109	37	66	95	1805		
GF 04.90/6				medium-K	54.48	1.08	16.54	7.10	0.05	9.19	4.57	4.72	1.97	0.30	99.14	173	25	922	45	104	22		176	268	54	19	177	62	895	8	
GF 04.90/7				high-K	69.90	0.49	15.03	2.34	0.03	1.39	2.05	4.02	4.57	0.18	99.69	25	187	23	478	118	33		50	47	86	20	78	79	760	2	
GF 04.90/10				medium-K	56.20	1.49	15.75	9.35	0.11	6.97	5.22	2.96	1.78	0.16	98.70	13	188	42	259	54	103	118	137	207	76		284	58	324	29	
GF 04.90/12				high-K	69.82	0.46	16.05	2.28	0.03	1.24	1.56	4.40	3.98	0.16	99.67	25	203	21	788	95	38		46	36	79	23	63	92	1211		
GF 04.90/13				high-K	75.84	0.14	13.54	0.91	0.02	0.33	0.45	3.89	4.84	0.05	100.08	18	96	15	214	115	10		34	21	35		23	61	401		
GF 04.90/14		2251 7206	quartz monzonite	medium-K	69.08	0.48	16.00	2.27	0.03	1.41	2.52	4.64	3.39	0.18	99.65	30	204	23	1018	86	41		43	33	61	30	73	78	1108	6	
GF 04.90/17	host	2251 7208		shoshonite	68.84	0.44	15.98	1.99	0.03	1.20	2.00	4.39	4.95	0.18	99.83	19	181	19	834	107	27		52	32	87	14	58	65	2076		
GF 10.90/1				high-K	56.28	1.54	16.80	6.74	0.19	4.32	5.51	5.50	2.25	0.88	98.71	60	379	32	940	90	97		54	24	19	176	55	236	73	383	19
GF 10.90/2				medium-K	57.46	1.23	15.97	7.20	0.18	5.98	5.30	5.00	1.39	0.29	98.88	61	313	34	810	38	200	10	87	290	174	62	201	67	222	28	
GF 10.90/3				medium-K	55.78	1.34	16.83	6.99	0.22	4.08	6.40	5.72	1.72	0.92	98.62	48	446	38	920	62	114	29	23	41	190	84	231	100	408	25	
GF 10.90/4				high-K	57.30	1.35	16.95	6.20	0.18	3.97	5.07	5.50	2.41	1.06	99.15	43	374	27	979	112	99		40		19	124	46	202	58	425	20
GF 10.90/5	host	2235 7168	granite	medium-K	71.76	0.37	15.79	1.70	0.10	1.36	2.23	3.87	2.68	0.15	99.77	22	210	30	1154	81	32		28	54	14	43	22	1060	3		
GF 10.90/6	host			medium-K	70.59	0.45	14.98	2.18	0.11	1.42	1.79	4.51	3.77	0.20	99.51	29	278	16	1003	91	24		27	60	74	42	1400	6			
GF 10.90/7				medium-K	72.11	0.28	15.17	1.37	0.11	0.83	1.48	4.94	3.59	0.12	99.63	22	279	10	1144	83	17		9	57		39	37	1774	7		
GF 10.90/8				medium-K	71.88	0.39	15.72	2.26	0.10	1.05	0.24	4.33	3.87	0.16	99.63	27	164	17	250	108	30		27	79		60	40	770	11		
GF 10.90/9				high-K	59.79	0.81	18.06	5.91	0.10	2.19	5.44	4.28	3.04	0.37	99.40	20	284	22	692	113	68	139	48	101	87	30	165	37	689	18	
GF 10.90/10	host	2270 7178	granite	shoshonite	76.18	0.10	13.24	0.71	0.05	0.21	0.78	2.89	5.81	0.03	99.82	19	106	9	329	117			7	20	16		16		531	2	
GF 10.90/11				shoshonite	57.30	1.19	17.64	7.45	0.18	4.34	4.18	4.12	3.49	0.12	99.15	27	537	18	687	176	108	576	79	155	73		198	45	881	23	
GF 10.90/12				shoshonite	56.21	1.24	18.53	7.03	0.20	3.59	6.54	1.84	4.54	0.27	99.07	15	172	21	346	126	89	34	151	247	69	28	182	24	489	22	
GF 10.90/14	host			high-K	66.46	0.59	16.40	3.02	0.14	1.68	3.30	4.80	3.36	0.26	99.66	33	336	17	1228	75	42		39	79		90	45	1698	9		
GF 10.90/15	host	2228 7176	granodiorite	medium-K	63.99	0.85	17.36	4.09	0.14	2.77	3.34	4.83	2.28	0.35	99.55	32	356	18	1403	74	53		28	54	74	42	138	28	795	5	
GF 10.90/16	host	2228 7175	quartz monzonite	medium-K	68.76	0.47	16.02	2.29	0.09	1.30	2.81	4.48	3.57	0.21	99.61	28	304	14	1137	91	39</										

GF 10.89/5B	enclave	2252 7173	monzodiorite	medium-K	53.70	1.44	14.67	7.27	0.23	9.86	6.63	4.09	1.77	0.34	99.06	87	203	28	626	78	135	11	189	413	88	307	197	21			
GF 10.89/5E	enclave	2252 7173		shoshonite	59.40	1.06	17.35	4.33	0.09	3.20	4.07	5.02	4.43	1.05	99.31	120	264	37	975	142	75	47	46	174	56	240	59	962	8		
GF 10.89/5F	enclave	2252 7173		high-K	61.83	0.61	16.08	3.98	0.09	4.08	4.77	4.83	3.52	0.21	99.14	95	162	21	927	75	57	94	220	49	144	20	892	16			
GF 10.89/5G	enclave	2252 7173		shoshonite	58.25	0.81	15.01	5.25	0.22	6.02	5.23	3.11	5.62	0.49	98.94	53	218	26	837	139	79	173	349	132	46	207	30	1380	7		
GF 10.89/5H	enclave	2252 7173	monzonite	medium-K	56.69	1.04	15.42	6.64	0.25	7.80	5.09	4.75	1.96	0.35	98.90	44	197	28	706	93	130	47	147	330	106	0	244	18	169	17	
GF 12.89/12A	enclave	2228 7175		shoshonite	55.98	1.59	13.56	9.44	0.21	4.37	4.53	3.97	6.18	0.16	98.80	30	386	23	1203	306	204	93	215	150	34	318	1823	6			
GF 12.89/12B	enclave	2228 7175	gabbroic diorite	medium-K	54.55	1.36	10.97	9.36	0.22	9.71	8.60	3.30	1.43	0.50	99.20	32	284	37	621	55	154	8	220	667	62	32	229	27	344	21	
GF 12.89/12C	enclave	2228 7175		high-K	57.12	1.46	17.54	6.88	0.08	3.35	4.80	5.27	2.47	1.02	98.62	55	329	47	823	128	109	25	38	2	147	48	235	66	302	7	
GF 12.89/12D	enclave	2228 7175		shoshonite	56.25	1.77	17.24	7.46	0.09	3.70	4.52	4.86	3.26	0.84	98.61	73	383	37	734	155	110	5	29	16	100	291	58	399			
GF 04.90/16A	enclave			high-K	55.54	1.20	14.89	6.62	0.10	7.92	6.63	3.97	2.68	0.43	98.90	20	229	33	1014	84	78	81	103	294	100	22	215	69	1065	32	
GF 04.90/16B	enclave	2251 7206	monzonite	medium-K	56.98	1.53	17.45	6.36	0.13	3.27	4.90	5.96	2.10	1.31	99.13	71	320	38	865	108	81	6	53	16	202	57	198	144	295		
GF 04.90/16C	enclave	2251 7206	monzodiorite	high-K	56.05	1.07	15.17	6.44	0.20	7.30	6.61	4.30	2.59	0.26	98.89	24	198	24	638	75	110	209	448	105	17	162	107	860	29		
GF 10.90/5	enclave	2235 7168	syenite	shoshonite	62.02	0.89	17.11	3.89	0.16	1.96	3.65	5.14	4.62	0.56	99.43	49	350	21	1050	121	61	423	22	114	47	135	57	1177	7		
GF 10.90/6	enclave	2257 7173		high-K	54.69	1.87	17.55	8.06	0.17	6.01	2.85	5.02	2.56	1.22	98.50	60	378	37	808	121	127	47	4	268	140	252	201	4832	17		
GF 10.90/10	enclave	2270 7178		medium-K	61.24	0.85	10.97	5.97	0.10	2.04	4.73	4.65	1.94	0.50	99.43	37	399	27	593	123	77	95	33	71	88	37	172	46	235	18	
GF 10.90/14	enclave			shoshonite	56.81	1.30	16.31	7.99	0.18	3.77	4.81	3.67	4.23	0.92	98.31	4	436	28	969	88	100	23	23	88	147	65	239	63	3046	30	
GF 10.90/15E	enclave	2228 7176	monzodiorite/monzonite	shoshonite	52.19	1.95	15.98	9.13	0.21	8.24	5.46	3.39	2.46	0.98	99.10	55	456	46	960	89	128	93	234	167	90	301	46	708	34		
GF 06.91/4A	enclave	2252 7173		high-K	57.85	1.04	16.86	5.51	0.28	5.13	5.16	5.20	2.60	0.37	99.07	39	499	24	1207	113	101	62	98	115	34	143	47	1075	9		
GF 06.91/5	enclave			medium-K	52.42	1.82	17.11	9.57	0.23	10.09	2.32	4.56	1.28	0.59	99.90	47	391	29	738	57	145	116	295	213	75	229	76	225	18		
GF 06.91/7A	enclave			high-K	53.36	1.49	14.47	6.63	0.26	10.96	5.97	4.07	2.30	0.48	99.46	42	440	23	954	117	97	23	166	357	121	37	215	43	571	32	
GF 06.91/7B	enclave	2252 7176	monzonite	high-K	56.74	1.22	17.20	5.81	0.21	4.82	5.29	5.63	2.40	0.67	98.88	34	664	28	1651	98	84	62	63	128	30	186	54	599	12		
GF 06.91/7C	enclave	2252 7176	gabbroic diorite	medium-K	55.41	2.20	14.17	10.07	0.21	7.63	4.74	4.01	1.12	0.42	97.92	49	247	23	168	100	147	106	186	137	48	285	71	966	12		
GF 06.91/7D	enclave	2252 7176	monzodiorite	medium-K	56.75	1.10	16.85	6.09	0.23	4.95	5.68	5.13	2.18	1.02	98.55	44	542	36	1089	114	102	22	39	36	181	57	177	73	306	24	
GF 06.91/7E	enclave	2252 7176	monzonite	medium-K	61.12	0.94	16.68	4.67	0.21	3.88	4.35	5.09	2.74	0.32	98.47	29	434	23	1012	101	80	24	57	42	31	140	70	578	15		
GF 06.91/7F	enclave	2252 7176	monzodiorite	high-K	52.36	1.31	13.67	6.85	0.30	10.96	7.21	3.81	2.12	1.42	99.76	35	352	18	681	103	113	195	509	163	63	205	83	552	20		
Garrabal Hill																															
GF 04.90/1		2259 7134		medium-K	52.63	1.03	12.48	12.12	0.20	9.86	7.10	2.66	1.64	0.29	99.03		167	31	676	66	92	8	222	676	40	206	84	430	30		
GH 04.90/19	host			medium-K	63.77	0.67	16.23	4.68	0.05	3.25	4.55	3.84	2.75	0.20	99.35	20	219	29	550	74	67	7	79	156	91	42	127	86	632		
GH 04.90/20	host	2305 7189	granodiorite	medium-K	63.70	0.64	16.44	4.39	0.06	3.19	4.63	3.97	2.78	0.19	99.38	11	203	24	549	85	57	4	81	145	98	76	134	68	702	2	
GH 04.90/21	host			high-K	62.64	0.66	16.10	5.01	0.06	4.18	4.25	3.84	3.10	0.17	99.05	14	184	25	670	120	55	30	102	212	58	119	63	688	4		
DRR 129.2		22593 71358	monzodiorite	medium-K	54.95	1.07	15.77	7.62	0.15	7.15	7.41	3.56	2.00	0.32	96.96	9	108	20	359	51.4	83	86	95	366	27	22.3	181	21	641	24	
DRR 130		22582 71366	f.grained u.mafic rock		41.06	0.13	0.47	18.54	0.15	39.56	0.03	0.02	0.01	0.02	86.88	< 1	2	< 1	4.63	1.14	73	3	1063	3675	< 3	0.46	80	< 3	2	13	
DRR 132		22582 71371	f.grained u.mafic rock		43.41	0.97	3.89	16.59	0.28	26.30	8.12	0.30	0.11	0.01	92.43	< 1	18	14	94.1	3.65	128	170	821	1457	< 3	8.76	258	< 3	59	42	
GH 04.90/18	enclave	2305 7189	diorite	medium-K	58.26	0.78	14.91	5.94	0.07	9.38	5.83	2.96	1.70	0.17	99.02	6	169	28	498	66	63	18	252	531	77	32	163	67	471	29	
GH 04.90/22	enclave			medium-K	58.69	0.77	15.06	5.72	0.05	8.78	5.54	3.18	2.05	0.17	99.00		163	26	498	82	71	5	238	52	23	155	92	498	12		
Arrochar																															
ARR 09.89/11		2276 7084	diorite	medium-K	61.68	0.74	16.33	5.70	0.11	3.99	5.02	4.43	1.80	0.19	98.99	8	239	29	540	47	71	8	54	124	0	127	27	575	16		
ARR 9.89/20		2268 7074	granodiorite	medium-K	69.10	0.34	16.89	2.10	0.06	1.17	2.36	5.37	2.45	0.15	99.92	13	188	17	597	49	56		11	30	36	21	708	7			
ARR 10.89/1				medium-K	55.31	0.94	16.51	7.61	0.13	7.23	7.51	2.75	1.80	0.21	98.92	233	30	393	51	80	54	76	198	32	215	25	411	22			
ARR 10.89/12				medium-K	54.88	0.91	15.80	7.62	0.15	7.57	7.93	3.21	1.71	0.22	98.88	156	33	439	49	81	47	125	314	39	14	194	20	388	32		
ARR 10.89/13				high-K	70.90	0.37	15.38	2.10	0.03	1.35	2.37	3.39	3.98	0.14	99.77	214	25	381	86					22	26	48	32	29	812	3	
ARR 10.89/16		22677 077		medium-K	46.30	0.92	9.05	11.46	0.21	21.03	9.73	0.83	0.36	0.10	98.46	89	22	228				90	15	885	1985	209	12	65	42		
ARR 10.89/17					53.11	0.46	1.48	14.69	0.18	27.37	2.42	0.22	0.04	0.02	98.20							119	256	747	2202	201	4				
ARR 10.89/19					41.29	0.13	0.57	15.71	0.16	41.23	0.63	0.21	0.03	0.02	97.69							75	1051	1628	73						
ARR 10.89/21				medium-K	69.37	0.34	16.98	2.46	0.06	1.30	2.95	4.29	2.08	0.16	99.68	274	22	595	47	49	13	19	30	44	3	5	22	614	10		
ARR 12.89/1				medium-K	50.96	0.75	11.30	12.90	0.21	11.46	8.74	2.79	0.68	0.21	98.81	71	35	188	25	111	51	229	546	23	186						
ARR 12.89/2		2264 7071		medium-K	55.07	1.01	16.80	7.77	0.16	6.28	7.94	2.91	1.80	0.26	98.78	135	29	497	45	74	55	61	150	50	11	224	21	429	64		
ARR 12.89/3		22687 072		medium-K	40.71	0.09	0.48	15.41	0.15	42.88	0.19	0.03	0.03	0.02	97.86							75	1512	2662	59						
ARR 12.89/4		2268 7072			44.71	0.39	1.52	12.91	0.23	28.56	11.38	0.22	0.05	0.02	98.91	27	15	19				94	877	2564	174						
ARR 12.89/5		2288 7071			48.76	0.37	1.46	12.11	0.22	23.93	12.88	0.23	0.04	0.01	100.31	31	23	14				78	542	2081	188						

<i>ARR 04.90/3</i>		2271 7080	<i>gabbro</i>	<i>medium-K</i>	48.69	1.48	8.89	11.20	0.20	16.73	10.16	1.23	1.26	0.14	98.48	8	131	39	181	28	97		489	1695	43		348	36	176	47	
<i>ARR 04.90/4</i>				<i>medium-K</i>	50.71	1.34	16.12	9.52	0.17	8.78	9.84	2.63	0.65	0.24	98.77	10	90	29	508		87	31	109	359	19		314	83	154	52	
<i>ARR 04.90/5</i>	<i>host</i>	2272 7081	<i>monzodiorite</i>	<i>high-K</i>	54.18	0.85	15.01	6.24	0.21	9.81	7.23	4.16	2.05	0.26	99.15	16	199	44	726	79	63	51	115	378	58	11	179	37	382	24	
<i>ARR 04.90/6</i>				<i>medium-K</i>	71.13	0.34	16.55	2.50	0.05	1.13	1.00	4.30	2.86	0.14	99.72	15	186	20	309	82	46	44	36	31	58		41	81	424		
<i>ARR 04.90/7</i>				<i>high-K</i>	51.82	1.03	14.42	9.10	0.18	11.07	7.74	2.49	1.96	0.19	98.41	101	29	89	67	83	36	204	611	53			241	39	182	13	
<i>ARR 04.90/8</i>				<i>medium-K</i>	69.44	0.32	16.91	2.23	0.04	1.09	2.96	4.33	2.54	0.14	99.70	13	167	17	624	57	50		34	29	90		54	92	543	1	
<i>ARR 04.90/9</i>				<i>low-K</i>	50.25	1.13	16.12	9.30	0.18	9.73	10.56	2.25	0.27	0.20	98.84		45	21	497		91	104	102	365			271	61		47	
<i>ARR 10.90/18</i>		2243 7060		<i>medium-K</i>	65.92	0.91	16.32	9.80	0.12	3.39	0.13	0.84	2.37	0.18	98.45	22	227	27		98	129	48	64	150	105	35	160	52	282	17	
<i>ARR 10.90/18A</i>		2243 7060		<i>high-K</i>	64.67	0.96	17.20	6.71	0.15	2.23	0.94	3.66	3.30	0.18	99.19	40	292	37	205	104	121	114	51	126	156	57	211	65	1334	21	
<i>ARR 10.90/19</i>	<i>dyke</i>	2296 7058	<i>gabbroic diorite</i>	<i>medium-K</i>	55.60	1.24	16.57	8.28	0.19	5.10	7.72	4.30	0.79	0.21	98.87	10	268	27	726	23	92	30		21	56		256	33	510	34	
<i>DRR 103</i>		23418 70958	<i>gabbroic diorite</i>	<i>medium-K</i>	57.12	1.00	16.35	7.46	0.15	5.49	7.15	3.09	2.03	0.16	97.48	8	129	21	430	54.5	78	71	37	131	26	18.5	207	18	448	25	
<i>DRR 108</i>		23438 71546	<i>gabbroic diorite</i>	<i>medium-K</i>	55.93	1.00	15.55	8.32	0.17	7.07	7.00	3.34	1.47	0.17	96.16	6	113	20	409	35.8	76	54	56	195	18	16.7	219	11	341	28	
<i>DRR 110</i>		23430 71504	<i>diorite</i>	<i>medium-K</i>	59.09	0.81	16.58	6.37	0.15	4.77	6.44	3.80	1.77	0.22	96.48	9	143	18	496	44.1	71	20	29	121	27	20.3	139	16	435	19	
<i>DRR 112</i>		23525 71463	<i>monzodiorite</i>	<i>shoshonite</i>	56.02	1.34	15.91	8.82	0.15	4.83	5.80	3.20	3.52	0.42	95.30	10	171	28	474	64.9	71	78	23	74	28	26.7	261	22	708	27	
<i>DRR 115</i>		23419 71431	<i>granodiorite</i>	<i>high-K</i>	67.63	0.43	16.03	3.61	0.06	1.78	2.96	3.78	3.54	0.17	97.34	9	162	10	567	83.9	29	3	14	42	37	18.1	58	25	705	7	
<i>ARR 04.90/5</i>	<i>enclave</i>	2272 7081	<i>gabbroic diorite</i>	<i>medium-K</i>	52.75	1.23	12.06	8.45	0.19	12.80	8.59	2.24	1.52	0.17	98.98	16	130	44	606	61	92	21	275	804	69	20	233	21	262	32	
<i>Ardhni</i>																															
<i>ARD 09.89/1</i>	<i>dyke</i>			<i>shoshonite</i>	55.37	1.15	18.46	8.83	0.15	3.65	6.87	1.96	3.35	0.21	99.05	19	225	41	374	119	113	8		32	79	21	300		560	37	
<i>ARD 09.89/2</i>		2317 7147	<i>gabbro</i>	<i>medium-K</i>	51.89	1.15	12.86	8.93	0.19	11.85	9.11	2.50	1.31	0.21	99.01	13	164	20	557	43	80	69	128	587	52	26	234	22	223	34	
<i>ARD 09.89/3</i>				<i>high-K</i>	58.29	0.96	17.42	5.92	0.16	4.02	5.76	4.12	3.03	0.33	99.13	16	255	26	745	11	69	256	47	101	82	33	186	34	790	22	
<i>ARD 09.89/5</i>				<i>medium-K</i>	70.59	0.34	15.73	2.39	0.13	1.20	2.42	3.87	3.19	0.13	99.84	20	233	14	697	91	51	13		9	61		52	27	900	8	
<i>ARD 09.89/6</i>				<i>high-K</i>	53.14	0.15	15.81	7.85	0.19	10.81	7.06	2.65	2.16	0.17	98.47	16	152	19	556	75	78	228	109	363	28		261	32	329	38	
<i>country rock</i>																															
<i>GF 07.91/5</i>		2272 7143	<i>pelitic schist</i>		64.58	1.28	16.49	7.97	0.18	3.85	0.55	0.73	4.25	0.13	99.30	65	276	64	167	164	107	33	74	159	148	59	175	65	868	14	

Notes:

sample numbers in *italics* indicate rocks used for Rb-Sr and Sm-Nd isotope analysis

'host' means rock containing analysed enclaves

coordinate system for grid references is the British Ordnance Survey National Grid, the prefix letters being NN

rocks named according to the scheme of Middlemost (1994)

major oxide concentrations in wt% normalised to 100% volatile-free, original XRF totals given

FeO* = total Fe as FeO

Mg# = 100Mg/(Mg+Fe)

trace element concentrations in ppm by weight

blank values indicate 'not analysed'

Table 2

Isotope data															
sample	comment	grid reference	rock name	Rb (ppm)	Sr (ppm)	Rb/Sr	⁸⁷ Rb/ ⁸⁶ Sr	⁸⁷ Sr/ ⁸⁶ Sr	⁸⁷ Sr/ ⁸⁶ Sr ₂₃₅	Sm (ppm)	Nd (ppm)	¹⁴⁷ Sm/ ¹⁴⁴ Nd	¹⁴² Nd/ ¹⁴⁴ Nd	εNd ₂₃₅	T _{DM} (Ga)
Glen Fyne															
GF 12.89/2		2252 7172	granite	80.7	1181	0.0684	0.1979	0.705305	0.704107	2.74	16.5	0.1002	0.512294	-1.5	1.29
GF 10.89/6		22625 71775	monzonite	97.4	538	0.1810	0.5238	0.709702	0.706531	4.53	24.1	0.1135	0.512312	-1.8	1.32
GF 04.90/14		2251 7206	quartz monzonite	79.4	888	0.0894	0.2586	0.705976	0.704411	3.86	22.5	0.1034	0.512294	-1.6	1.30
GF 10.90/5		2235 7168	granite	69.2	903	0.0767	0.2219	0.705784	0.704441	2.49	14.7	0.1026	0.512312	-1.3	1.27
GF 10.90/10		2270 7178	granite	126	246	0.5114	1.4805	0.714031	0.705069	0.33	2.03	0.0988	0.512237	-2.5	1.37
GF 10.90/15		2228 7176	granodiorite	59.1	1096	0.0539	0.1559	0.706627	0.705683	6.33	34.0	0.1124	0.512340	-1.2	1.27
GF 10.90/16		2228 7175	quartz monzonite	82.2	928	0.0885	0.2560	0.705987	0.704437	3.92	22.9	0.1034	0.512295	-1.6	1.30
GF 06.91/4A		2252 7173	quartz monzonite	66.6	1127	0.0591	0.1710	0.705681	0.704646	3.87	22.6	0.1037	0.512320	-1.1	1.26
GF 06.91/7F		2252 7176	granodiorite	66.5	1156	0.0575	0.1663	0.705342	0.704335	3.82	22.3	0.1036	0.512310	-1.3	1.28
GF 06.91/9		2229 7160	quartz monzonite	69.5	1039	0.0669	0.1935	0.705810	0.704639	4.87	28.0	0.1051	0.512306	-1.5	1.29
GF 02.92/23		22660 71785	monzonite	109	523	0.2081	0.6022	0.710370	0.706724	4.32	22.4	0.1168	0.512340	-1.5	1.29
GF 02.92/24		2263 7177	granite	83.2	262	0.3172	0.9181	0.711532	0.705975	0.63	3.99	0.0947	0.512191	-3.2	1.42
GF 10.89/5B	enclave	2252 7173	monzodiorite	82.3	564	0.1460	0.4224	0.706909	0.704352	8.34	49.7	0.1014	0.512379	0.1	1.16
GF 10.89/5H	enclave	2252 7173	monzonite	76.7	632	0.1213	0.3509	0.706306	0.704182	5.41	32.0	0.1023	0.512341	-0.7	1.22
GF 12.89/12B	enclave	2228 7175	gabbroic diorite	56.4	555	0.1017	0.2942	0.706633	0.704852	11.1	58.4	0.1146	0.512320	-1.7	1.31
GF 04.90/16B	enclave	2251 7206	monzonite	91.8	710	0.1293	0.3741	0.706932	0.704668	11.0	66.4	0.1000	0.512345	-0.5	1.20
GF 04.90/16C	enclave	2251 7206	monzodiorite	75.9	551	0.1377	0.3984	0.707219	0.704807	5.95	35.0	0.1026	0.512395	0.4	1.13
GF 10.90/5E	enclave	2235 7168	syenite	124	804	0.1543	0.4464	0.707094	0.704392	8.21	50.7	0.0979	0.512383	0.4	1.13
GF 10.90/15E	enclave	2228 7176	monzodiorite/monzonite	66.1	914	0.0723	0.2092	0.707249	0.705983	17.9	90.5	0.1197	0.512355	-1.3	1.27
GF 06.91/7B	enclave	2252 7176	monzonite	89.0	1302	0.0684	0.1979	0.705740	0.704542	7.68	43.5	0.1067	0.512364	-0.5	1.20
GF 06.91/7C	enclave*	2252 7176	gabbroic diorite	91.2	117	0.7797	2.2575	0.714995	0.701330	6.78	43.0	0.0953	0.512381	0.5	1.12
GF 06.91/7D	enclave (whole)	2252 7176	monzodiorite	105	877	0.1197	0.3463	0.706776	0.704680	12.3	70.6	0.1055	0.512329	-1.1	1.25
GF 06.91/7D	enclave (core)*	2252 7176	monzodiorite	144	892	0.1615	0.4672	0.707427	0.704599	13.8	76.7	0.1086	0.512329	-1.2	1.27
GF 06.91/7E	enclave	2252 7176	monzonite	97.8	793	0.1233	0.3567	0.706497	0.704338	5.42	31.7	0.1034	0.512331	-0.9	1.24
GF 06.91/7F	enclave	2252 7176	monzodiorite	101	558	0.1806	0.5225	0.707550	0.704387	10.2	59.9	0.1033	0.512376	0.0	1.17
Garabal Hill															
GH 04.90/20	host	2305 7189	granodiorite	69.5	502	0.1384	0.4005	0.710073	0.707649	3.89	20.4	0.1154	0.512254	-3.1	1.41
DDR 129.2		22593 71358	monzodiorite	51.4	559	0.0919	0.2659	0.709130	0.707520	4.72	22.3	0.1280	0.512419	-0.5	1.21
DDR 130		22582 71366	f.-grained ultramafic	1.1	5	0.2455	0.7108	0.714474	0.710171	0.14	0.5	0.1802	0.512561	-0.6	1.21
DDR 132		22582 71371	f.-grained ultramafic	3.7	94.1	0.0388	0.1123	0.707022	0.706343	2.80	8.76	0.1936	0.512680	1.0	1.08
GH 04.90/18	enclave	2305 7189	diorite	58.2	435	0.1338	0.3872	0.709528	0.707184	3.72	18.4	0.1225	0.512335	-1.9	1.32
Arrochar															
ARR 09.89/11		2276 7084	diorite	53.0	442	0.1199	0.3470	0.711191	0.709090	3.84	19.7	0.1178	0.512135	-5.5	1.60
ARR 09.89/20		2268 7074	granodiorite	51.2	545	0.0941	0.2723	0.709365	0.707717	1.93	11.5	0.1018	0.512276	-1.9	1.32
ARR 04.90/3		2271 7080	gabbro	32.1	161	0.1994	0.5771	0.710813	0.707320	5.82	24.5	0.1436	0.512469	-0.4	1.20
ARR 04.90/5	host	2272 7081	monzodiorite	66.1	554	0.1193	0.3453	0.711241	0.709151	4.37	19.7	0.1340	0.512245	-4.3	1.50
ARR 10.90/19	dyke	2296 7058	gabbroic diorite	26.9	517	0.0521	0.1508	0.711615	0.710702	4.77	21.9	0.1319	0.512389	-1.3	1.27
DDR 103		23418 70958	gabbroic diorite	54.5	430	0.1267	0.3668	0.713501	0.711281	4.00	18.5	0.1307	0.512173	-5.5	1.59
DDR 108		23438 71546	gabbroic diorite	35.8	409	0.0876	0.2536	0.712985	0.711450	3.89	16.7	0.1412	0.512459	-0.5	1.20
DDR 110		23430 71504	diorite	44.1	496	0.0890	0.2576	0.710755	0.709196	4.22	20.3	0.1258	0.512396	-0.9	1.24
DDR 112		23525 71463	monzodiorite	64.9	474	0.1368	0.3959	0.710761	0.708364	5.96	26.7	0.1349	0.512321	-2.8	1.39
DDR 115		23419 71431	granodiorite	83.9	567	0.1480	0.4283	0.710173	0.707580	3.16	18.1	0.1057	0.512160	-4.4	1.51
ARR 04.90/5	enclave	2272 7081	gabbroic diorite	52.8	469	0.1127	0.3262	0.712217	0.710242	4.71	20.2	0.1409	0.512323	-3.1	1.41
Ardlui															
ARD 09.89/2		2317 7147	gabbro	32.4	398	0.0815	0.2358	0.708981	0.707553	3.51	14.7	0.1442	0.512643	3.0	0.91
country rock															
GF 07.91/5		2272 7143	schist	122	94.6	1.2854	3.7316	0.742375	0.719787	7.84	41.9	0.1078	0.511775	-12.0	2.04

* not plotted in the diagrams